

DrugOOD: Out-of-Distribution (OOD) Dataset Curator and Benchmark for AI-aided Drug Discovery

– A Focus on Affinity Prediction Problems with Noise Annotations

Yuanfeng Ji^{1,3,*} Lu Zhang^{1,2,*} Jiayang Wu¹ Bingzhe Wu¹ Long-Kai Huang¹
Tingyang Xu¹ Yu Rong¹ Lanqing Li¹ Jie Ren¹ Ding Xue¹ Houtim Lai¹
Shaoyong Xu¹ Jing Feng¹ Wei Liu¹ Ping Luo³ Shuigeng Zhou²
Junzhou Huang¹ Peilin Zhao¹ Yatao Bian^{1†}

¹Tencent AI Lab, China

²Fudan University, China

³The University of Hong Kong, China

January 25, 2022

Abstract

AI-aided drug discovery (AIDD) is gaining increasing popularity due to its promise of making the search for new pharmaceuticals quicker, cheaper and more efficient. In spite of its extensive use in many fields, such as ADMET prediction, virtual screening, protein folding and generative chemistry, little has been explored in terms of the out-of-distribution (OOD) learning problem with *noise*, which is inevitable in real world AIDD applications.

In this work, we present DrugOOD¹, a systematic OOD dataset curator and benchmark for AI-aided drug discovery, which comes with an open-source Python package that fully automates the data curation and OOD benchmarking processes. We focus on one of the most crucial problems in AIDD: drug target binding affinity prediction, which involves both macromolecule (protein target) and small-molecule (drug compound). In contrast to only providing fixed datasets, DrugOOD offers automated dataset curator with user-friendly customization scripts, rich domain annotations aligned with biochemistry knowledge, realistic noise annotations and rigorous benchmarking of state-of-the-art OOD algorithms. Since the molecular data is often modeled as irregular graphs using graph neural network (GNN) backbones, DrugOOD also serves as a valuable testbed for *graph OOD learning* problems. Extensive empirical studies have shown a significant performance gap between in-distribution and out-of-distribution experiments, which highlights the need to develop better schemes that can allow for OOD generalization under noise for AIDD.

Keywords: AI-aided drug discovery (AIDD), graph OOD learning, OOD generalization, learning under noise, binding affinity prediction, drug-target interaction, virtual screening

*Equal contribution. Order was determined by tossing a coin.

†Correspondence to: Yatao Bian, email: DrugAIOOD@gmail.com

1. Project Page: <https://drugood.github.io>

Contents

1	Introduction	3
2	Background and Related Work	5
2.1	Binding Affinity Prediction in AI-aided Drug Discovery	6
2.1.1	Databases	6
2.1.2	Methods	7
2.1.3	Discussions	8
2.2	General OOD Databases	8
2.3	Benchmark Scheme	9
2.3.1	General Methods for OOD and Noisy Labels	9
2.3.2	Representation Learning for Affinity Prediction	11
3	Automated Dataset Curator with Real-world Domain and Noise Annotations	12
3.1	Filtering Data with Different Noise Levels	13
3.2	Processing Uncertainty and Multiple Measurements	14
3.3	Binary Classification Task with Adaptive Threshold	14
3.4	Domain Definition and Split	15
3.4.1	Domain Definition	15
3.4.2	Domain Split	15
3.5	Overview of the Dataset Curation Pipeline	17
4	Benchmarking State-of-the-art OOD Algorithms	17
4.1	Architecture Design	18
4.2	Domain Generalization Algorithms	19
5	Implementations and Package Usage	21
5.1	Dataset Curation	22
5.2	Dataset Loading	23
5.3	Algorithm Configuration	24
6	Empirical Studies	25
6.1	Ligand Based Affinity Prediction (LBAP)	25
6.1.1	Setup	25
6.1.2	Baseline Results	28
6.1.3	Performance Drops of Different Domains	30
6.1.4	Performance Drops of Different Noise Levels	30
6.2	Structure Based Affinity Prediction (SBAP)	31
6.2.1	Setup	31
6.2.2	Model	31
6.2.3	Baseline Results	31
6.2.4	Performance Gap of Different Domains	32
6.2.5	Study for Different Noise Levels	33
6.2.6	Study for Different Measurement Types	34
7	Discussions and Future Work	34
A	Statistics of the Realized Datasets	51

1. Introduction

The traditional drug discovery process is extremely time-consuming and expensive. Typically, the development of a new drug takes nearly a decade and costs about \$3 billion (Pushpakom et al., 2019), whereas about 90% of experimental drugs fail during lab, animal or human testing. Meanwhile, the number of drugs approved every year per dollar spent on development has plateaued or decreased for most of the past decade (Nosengo, 2016). To accelerate the development for new drugs, drugmakers and investors turn their attention to artificial intelligence (Muratov et al., 2020) techniques for drug discovery, which aims at rapidly identifying new compounds and modeling complex mechanisms in the body to automate previously manual processes (Schneider, 2018).

The applications of AI aided drug discovery is being continuously extended in the pharmaceutical field, ranging from ADMET prediction (Wu et al., 2018; Rong et al., 2020), target identification (Zeng et al., 2020; Mamoshina et al., 2018), protein structure prediction and protein design (Jumper et al., 2021; Baek et al., 2021; Gao et al., 2020), retrosynthetic analysis (Coley et al., 2017; Segler et al., 2018; Yan et al., 2020a), search of antibiotics (Stokes et al., 2020), generative chemistry (Sanchez-Lengeling et al., 2017; Simonovsky & Komodakis, 2018), drug repurposing for emerging diseases (Gysi et al., 2021) to virtual screening (Hu et al., 2016; Karimi et al., 2019; Lim et al., 2019). Among them, virtual screening is one of the most important yet challenging applications. The aim of virtual screening is to pinpoint a small set of compounds with high binding affinity for a given target protein in the presence of a large number of candidate compounds. A crucial task in solving the virtual screening problem is to develop computational approaches to predict the binding affinity of a given drug-target pair, which is the main task studied in this paper.

In the field of AI-aided drug discovery, the problem of *distribution shift*, where the training distribution differs from the test distribution, is ubiquitous. For instance, when performing virtual screening for hit finding, the prediction model is typically trained on known target proteins. However, a "black swan" event like COVID-19 can occur, resulting in a new target with unseen data distribution. The performance on the new target will significantly degrades. To handle the performance degradation (Koh et al., 2021) caused by distribution shift, it is essential to develop robust and generalizable algorithms for this challenging setting in AIDD. Despite its importance in the real-world problem, curated OOD datasets and benchmarks are currently lacking in addressing generalization in AI-aided drug discovery.

Another essential issue in the field of AI-aided drug discovery is the label noise. The AI model are typical trained on public datasets, such as ChEMBL, whereas the bioassay data in the dataset are often noisy (Kramer et al., 2012; Cortés-Ciriano & Bender, 2016). For example, the activity data provided in ChEMBL is extracted manually from full text articles in seven Medicinal Chemistry journals (Mendez et al., 2019). Various factors can cause noise in the data provided in ChEMBL, including but not limited to different confidence levels for activities measured through experiments, unit-transcription errors, repeated citations of single measurements and different "cut-off" noise². Figure 1 shows

2. E.g., measurements could be recorded with $<$, \leq , \approx , $>$, \geq etc, which would introduce the "cut-off" noise when translated into supervision labels.

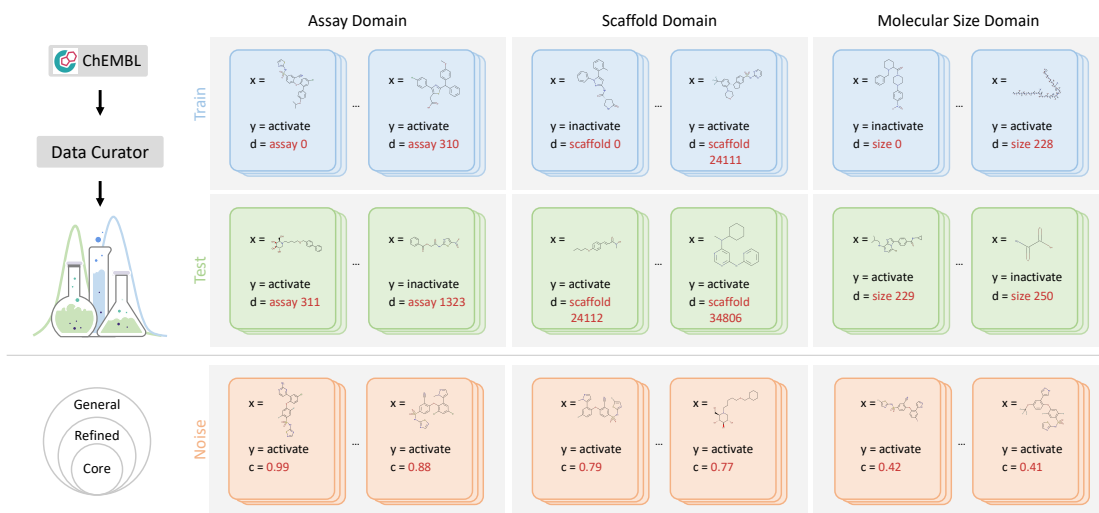


Figure 1: Drug00D provides large-scale, realistic, and diverse datasets for Drug AI OOD research. Specifically, Drug00D focuses on the problem of domain generalization, in which we train and test the model on disjoint domains, e.g., molecules in a new assay environment. *Top Left*: Based on the ChEMBL database, we present an automated dataset curator for customizing OOD datasets flexibly. *Top Right*: Drug00D releases realized exemplar datasets spanning different domain shifts. In each dataset, each data sample (x, y, d) is associated with a domain annotation d . We use the background colours blue and green to denote the seen data and unseen test data. *Bottom*: Examples with different noise levels from the Drug00D dataset. Drug00D identifies and annotates three noise levels (left to right: core, refined, general) according to several criteria, and as the level increases, data volume increases and more noisy sources are involved.

examples with different noisy levels. Meanwhile, real world data with noise annotations is lacking for learning tasks under noise labels (Angluin & Laird, 1988; Han et al., 2020).

To help accelerate research by focusing community attention and simplifying systematic comparisons between data collection and implementation method, we present Drug00D, a systematic OOD dataset curator and benchmark for AI-aided drug discovery which comes with an open-source Python package that fully automates the data curation process and OOD benchmarking process. We focus on the most challenging OOD setting: domain generalization (Zhou et al., 2021b) problem in AI-aided drug discovery, though Drug00D can be easily adapted to other OOD settings, such as subpopulation shift (Koh et al., 2021) and domain adaptation (Zhuang et al., 2020). Our dataset is also the first AIDD dataset curator with realistic noise annotations, that can serve as an important testbed for the setting of learning under noise.

Notably, we present an automated dataset curator based on the large-scale bioassay deposition website ChEMBL (Mendez et al., 2019), in contrast to just providing a set of curated datasets. Figure 2 gives an overview of the automated dataset curator. Using this dataset curator, potential researchers/practitioners can generate new OOD datasets based on their specific needs by simply re-configuring the curation process, i.e., modifying the

YAML files in the python package. Specifically, we also realize this dataset curator by generating 96 OOD datasets spanning various domains, noise annotations and measurement types. This mechanism comes with two advantages: i) It ensures that our released datasets and benchmarks are fully reproducible. ii) It allows great flexibility for future usage since it is often difficult, even for domain experts, to agree on one specific configuration. As an example, using EC50 as a measure of affinity, agreeing on a threshold for partitioning to find active/inactive pairs may be challenging.

As OOD learning subsumes or is closed related to other learning settings with distribution shift, such as domain adaption (Zhuang et al., 2020), transfer learning (Pan & Yang, 2009), and zero-shot learning (Romera-Paredes & Torr, 2015; Wang et al., 2019b), DrugOOD can also serve as a benchmark dataset or be used to generate datasets to study affinity prediction problems in AIDD under these learning settings. The following components summarize our major contributions:

1. *Automated Dataset Curator*: We provide a fully customizable pipeline for curating OOD datasets for AI-aided drug discovery from the large-scale bioassay deposition website ChEMBL.
2. *Rich domain annotations*: We present various approaches to generate specific domains that are aligned with the domain knowledge of biochemistry.
3. *Realistic noise annotations*: We annotate real-world noise according to the measurement confidence score, "cut-off" noise etc, offering a valuable testbed for learning under real-world noise.
4. *Rigorous OOD benchmarking*: We benchmark six SOTA OOD algorithms with various backbones for the 96 realized dataset instances and gain insight into OOD learning under noise for AIDD.

Paper Organizations. Section 2 presents background and related work on AI-aided drug discovery, existing OOD algorithms, datasets, benchmarks and affinity prediction-related materials. In Section 3 we provide details on the automated dataset curator with real-world domain and noise annotations. We present specifics on benchmarking SOTA OOD algorithms in Section 4. Section 5 gives implementation details and package usage guidelines. We present experimental results and corresponding discussions in Section 6. Lastly, Section 7 discusses and concludes the paper.

2. Background and Related Work

In this section, we review the current progress in binding affinity prediction problems, one of highly active research areas in AIDD. The performance of affinity prediction is often limited by OOD issues and noisy labels, which motivates us to propose the DrugOOD database to explicitly tackle such problems. Lastly, we summarize general methods for OOD and noisy labels, together with representation learning for affinity prediction for virtual screening, which are later used for benchmark tests on the DrugOOD datasets.

2.1 Binding Affinity Prediction in AI-aided Drug Discovery

The ability of AI techniques has been dramatically boosted in various domains, mainly due to wide-spread applications of deep neural networks. We have witnessed a growing number of researches attempting to solve traditional problems in the drug discovery with more advanced AI models. There have been several surveys (Sliwoski et al., 2013; Jing et al., 2018; Yang et al., 2019b; Paul et al., 2021; Deng et al., 2021; Bender & Cortés-Ciriano, 2021) summarizing recent advances and problems in this area, covering key aspects including major applications, representative techniques, and critical assessment benchmarks.

As pointed out in (Yang et al., 2019b; Paul et al., 2021), most of AI-driven applications can be roughly categorized into two domains, i.e., molecule generation and molecule screening. Molecule generation aims at adopting generative models to produce a large pool of candidate drug molecules with certain restraints satisfied (Simonovsky & Komodakis, 2018; Sanchez-Lengeling et al., 2017; Satorras et al., 2021). On the other hand, molecule screening attempts to identify the most promising molecule(s) based on a wide range of predicted properties (Yang et al., 2019a; Feinberg et al., 2020; Jiménez et al., 2018). Other typical applications of AI techniques in drug discovery include target identification (Zeng et al., 2020; Mamoshina et al., 2018), target structure prediction (Jumper et al., 2021; Baek et al., 2021), drug re-purposing (Aliper et al., 2016; Issa et al., 2021; Pham et al., 2021), and molecule retrosynthesis (Coley et al., 2017; Zheng et al., 2019; Chen et al., 2020).

For conducting virtual screening on candidate molecules, both target-independent (e.g. ADMET) and target-dependent (e.g. binding affinity) properties are critical. The former ones measure how likely the molecule itself is qualified as a candidate drug, for instance, it should not induce severe liver toxicity to human (Zhang et al., 2016; Asilar et al., 2020). On the other hand, target-dependent properties consider the tendency of its potential interaction with the target (and other unrelated proteins), which often heavily depends on the joint formulation of candidate molecule and target (Hu et al., 2016; Karimi et al., 2019; Lim et al., 2019). In this paper, we mainly concentrate on the binding affinity between molecule and protein target, which falls into the domain of predicting target-dependent properties. In this circumstance, the out-of-distribution issue may result in severe performance degradation (e.g., when the target distribution dramatically differs between model training and inference), which leads to the major motivation of this paper.

2.1.1 DATABASES

ChEMBL (Davies et al., 2015; Mendez et al., 2019) is a large-scale open-access database consists of small molecules and their biological activity data. Such information is mainly extracted from medicinal chemistry journal articles, supplemented with data collected from approved drugs and clinical development candidates. It now contains over 2.1 million distinct compounds and 18.6 million records of their activities, which involve over 14,500 targets.

BindingDB (Gilson et al., 2016) collects experimental interaction data between proteins and small molecules, primarily from scientific articles and US patents. BindingDB also gathers selected data entries from other related databases, including PubChem (Wang et al., 2009), ChEMBL (Mendez et al., 2019), PDSP Ki (Roth et al., 2000), and CSAR (Carl-

son & Dunbar Jr, 2011). Advanced search tools, hypothesis generation schemes (from targets to compounds and vice versa), and virtual compound screening methods are also integrated in the database.

PDBbind (Liu et al., 2014) is created to collect biomolecular complexes from the PDB database (Burley et al., 2020), with experimental binding affinity data curated from original reference papers. The latest release of PDBbind (version 2020) consists of over 23,000 biomolecular complexes, whose majority are protein-ligand complexes (19,443) and protein-protein complexes (2,852), and the remaining part are mainly protein-nucleic acid and nucleic acid-ligand complexes.

2.1.2 METHODS

It is often critical to access the target structure before estimating the affinity of candidate molecules, since the affinity is jointly determined by the interaction between molecule and target. Depending on the availability of known target structures, affinity prediction methods can be roughly divided into two categories: ligand-based and structure-based.

Ligand-based affinity prediction (LBAP). Based on the hypothesis that structurally analogous compounds tend to have similar biological activities (Johnson & Maggiora, 1990), ligand-based affinity prediction methods are developed. The ultimate goal is to identify promising compounds from a large candidate library, based on their similarities to known active compounds for an interested target. Several approaches are proposed to filter compounds based on chemical similarity measurements, e.g., Tanimoto coefficients (Kim & Skolnick, 2008) and similarity ensemble approach (SEA) (Keiser et al., 2007). Such methods heavily rely on hand-crafted or learnt compound representations, describing various properties including molecule weight, geometry, volume, surface areas, ring content, etc. On the other hand, quantitative structure-activity relationship (QSAR) based approaches attempt to explicitly formulate the relationship between structural properties of chemical compounds and their biological activities (Kwon et al., 2019). Various machine learning techniques have been cooperated with QSAR-based affinity prediction, including linear regression (Luco & Ferretti, 1997), random forest (Svetnik et al., 2003), support vector machine (Zakharov et al., 2016), and neural networks (Burden & Winkler, 1999; Pradeep et al., 2016). Particularly, multi-task neural networks (Dahl et al., 2014) alleviate the over-fitting issue by optimizing over multiple bioassays simultaneously, and was adopted to achieve the best performance in the Merck Molecular Activity Challenge³.

Despite the satisfying performance of ligand-based affinity prediction approaches in certain scenarios, they do not take target structures in consideration. However, the interaction between target and molecule is indeed essential in accurately predicting the binding affinity, which leads more and more researches to focus on structure-based affinity prediction.

Structure-based affinity prediction (SBAP). In contrast to ligand-based approaches, structure-based methods (Lim et al., 2021) usually take structures of protein targets and/or protein-ligand complexes as inputs for affinity prediction. Some work (Wallach et al.,

3. Merck Molecular Activity Challenge: <https://www.kaggle.com/c/MerckActivity>

2015; Li et al., 2021b) predicts the binding affinity from experimentally determined protein-ligand co-crystal structures, but such data is highly expensive and time-consuming to obtain in practice. Others turn to computation-based docking routines (Trott & Olson, 2010; Koes et al., 2013; McNutt et al., 2021; Bao et al., 2021) to estimate protein-ligand complex structures through sampling and ranking, and then formulate the structure-affinity relationship via various models.

Ballester & Mitchell (2010) propose the RF-Score approach to use random forest to implicitly capture binding effects based on a series of carefully designed hand-crafted features. 3D convolutional neural networks are adopted in (Stepniewska-Dziubinska et al., 2018; Jiménez et al., 2018), where protein-ligand complex structures are discretized into 3D voxels and then fed into the model for affinity prediction. However, such discretization fails to capture the 3D rotational and translational invariance of 3D structures, and thus relies on heavy data augmentation to overcome such limitations. Graph neural networks are adopted in Jiang et al. (2021) to simultaneously formulate the intra-molecular and inter-molecular interactions, where nodes correspond to ligand/protein atoms, and edges are defined by both covalent and non-covalent linkages.

2.1.3 DISCUSSIONS

For most machine learning based approaches, it is usually desirable that the data distribution of training and evaluation subsets are as close as possible. However, this often does not hold true for affinity prediction tasks, e.g., the scaffold of small molecules and/or family of protein targets encountered during inference may be unseen throughout the model training process. Simply dividing the database into training and evaluation subsets on a per target-molecule basis may lead to over-optimistic performance, which is unrealistic for real-world applications.

Nonetheless, most databases for experimental binding affinities do not provide an official data split or its generation pipeline for model training and evaluation. To make things even more complicated, binding affinity annotations could be highly noisy, due to different experimental settings, affinity measurements, and confidence scores. Researchers need to manually pre-process raw data entries and re-organize them into the standard format, which is not only laborious and burdensome, but also unfavorable for a fair comparison against existing baselines. Therefore, we propose DrugOOD as a highly customizable curator for OOD datasets with noisy labels explicitly considered, so as to promote more efficient development of affinity prediction approaches in AIDD.

2.2 General OOD Databases

The out-of-distribution issue has attracted an ever-growing research interest in recent years, due to its importance in improving the generalization ability in real-world applications. Several databases have been constructed with great emphasis placed on the out-of-distribution generalization performance, mainly consist of computer vision and natural language processing tasks.

In Koh et al. (2021), the WILDS benchmark is proposed to reflect various levels of distribution shifts that may occur in real-world scenarios. It considers two common types of distribution shifts: domain generalization and sub-population shift. A total of 10

datasets are included, covering shifts across cameras for wildlife monitoring, hospitals for tumor identification, users for product rating estimation, and *f* scaffolds for biochemical property prediction, etc. [Sagawa et al. \(2021\)](#) further extend this database to include unlabeled data for unsupervised domain adaptation.

DomainBed ([Gulrajani & Lopez-Paz, 2020](#)) consists of 7 multi-domain image classification datasets, including Colored MNIST ([Arjovsky et al., 2019](#)), Rotated MNIST ([Ghifary et al., 2015](#)), PACS ([Li et al., 2017](#)), VLCS ([Fang et al., 2013](#)), Office-Home ([Venkateswara et al., 2017](#)), Terra Incognita ([Beery et al., 2018](#)), and DomainNet ([Peng et al., 2019](#)). Furthermore, authors point out the importance of model selection strategy in the domain generalization task, and conduct thorough benchmark tests over 9 baseline algorithms and 3 model selection criteria. As it turns out, empirical risk minimization (ERM) ([Vapnik, 1999](#)) with a careful implementation achieves state-of-the-art performance across all datasets, even when compared against various domain generalization algorithms.

[Ye et al. \(2021\)](#) analyze the performance comparison between ERM and domain generalization algorithms on DomainBed, and point out that the distribution shift is composed of diversity shift and correlation shift, and existing domain generalization algorithms are only optimized towards one of them. They further propose additional datasets, of which WILDS-Camelyon17 ([Koh et al., 2021](#)) is dominated by diversity shift, and NICO ([He et al., 2021](#)) and CelebA ([Liu et al., 2015](#)) are dominated by correlation shift.

As described above, general OOD databases are mostly built with image and text data, with one exception being the ODGB-MolPCBA dataset from WILDS ([Koh et al., 2021](#)), which aims at predicting biochemical properties from molecular graphs. The distribution shift is mainly caused by disjoint molecular scaffolds between training and test subsets. This is indeed critical for accurate prediction of target-independent properties, but is still insufficient for affinity prediction where the target information should be explicitly exploited. TDC ([Huang et al., 2021](#)) as another concurrent AIDD benchmark, offers SBAP datasets collated from BindingDB with a temporal split by patent year between 2013-2021, which is still limited in scope for drug OOD problems. In contrast, DrugOOD covers comprehensive sources of out-of-distribution in affinity prediction, and provides a dataset curator for highly customizable generation of OOD datasets. Additionally, noisy annotations are taken into consideration, so that algorithms can be evaluated in a more realistic setting, which further bridges the gap between researches and pharmaceutical applications.

2.3 Benchmark Scheme

In addition to an automated dataset curator in DrugOOD, we also provide rigorous benchmark tests over state-of-the-art OOD algorithms, with graph neural networks and BERT-like models used for representation learning from structural and sequential data. Next, we briefly review these OOD and representation learning algorithms, while more detailed descriptions can be found in [Section 4](#).

2.3.1 GENERAL METHODS FOR OOD AND NOISY LABELS

The out-of-distribution and noisy label issues have been extensively studied in the machine learning community, due to their importance in improving the generalization ability

and robustness. Here, we summarize recent progress in these two areas respectively, with a few overlaps since some approaches are proposed to jointly tackle these two issues in one shot.

Methods for OOD. To improve the model generalization ability over out-of-distribution test samples, some work focuses on aligning feature representations across different domains. The minimization of feature discrepancy can be conducted over various distance metrics, including second-order statistics (Sun & Saenko, 2016), maximum mean discrepancy (Tzeng et al., 2014) and Wasserstein distance (Zhou et al., 2021b), or measured by adversarial networks (Ganin et al., 2016). Others apply data augmentation to generate new samples or domains to promote the consistency of feature representations, such as Mixup across existing domains (Xu et al., 2020; Yan et al., 2020b), or in an adversarial manner (Zhao et al., 2020; Qiao et al., 2020).

With the label distribution further taken into consideration, recent work aims at enhancing the correlation between domain-invariant representations and labels. For instance, invariant risk minimization (Arjovsky et al., 2019) seeks for a data representation, so that the optimal classifier trained on top of this representation matches for all domains. Additional regularization terms are proposed to align gradients across domains (Koyama & Yamaguchi, 2021), reduce the variance of risks of all domains (Krueger et al., 2021b), or smooth inter-domain interpolation paths (Chuang & Mroueh, 2021).

Methods for noisy labels. There is a rich body of literature trying to combat with the label-noise issue, starting from the seminal work (Angluin & Laird, 1988) for traditional statistical learning to recent work for deep learning (Han et al., 2018b, 2019; Song et al., 2020a). Generally speaking, previous methods attempt to handle noisy labels mainly from three aspects (Han et al., 2020): training data correction (van Rooyen et al., 2015; van Rooyen & Williamson, 2017), objective function design (Azadi et al., 2016; Wang et al., 2017), and optimization algorithm design (Jiang et al., 2018; Han et al., 2018b).

From the training data perspective, prior work (van Rooyen & Williamson, 2017) firstly estimates the noise transition matrix, which characterizes the relationship between clean and noisy labels, and then employs the estimated matrix to correct noisy training labels. Typical work in this line includes using an adaptation layer to model the noise transition matrix (Sukhbaatar et al., 2015), label smoothing (Lukasik et al., 2020), and human-in-the-loop estimation (Han et al., 2018a).

Other work turns to the design of objective functions, which aims at introducing specific regularization into the original empirical loss function to mitigate the label noise effect. In Azadi et al. (2016), authors propose a group sparse regularizer on the response of image classifier to force weights of irrelevant or noisy groups towards zero. Zhang et al. (2017) introduce Mixup as an implicit regularizer, which constructs virtual training samples by linear interpolation between pairs of samples and their labels. Such approach not only regularizes the model to factor simple linear behavior, but also alleviates the memorization of corrupted labels. Similar work following this idea includes label ensemble (Laine & Aila, 2017) and importance re-weighting (Liu & Tao, 2015).

From the view of optimization algorithm design, some work (Han et al., 2018b; Li et al., 2020) introduces novel optimization algorithms or schedule strategies to solve the label noise issue. One common approach in this line is to train a single neural network

via small loss tricks (Ren et al., 2018; Jiang et al., 2018). Besides, other work proposes to co-train two neural networks via small-loss tricks, including co-teaching (Han et al., 2018b) and co-teaching+ (Yu et al., 2019).

2.3.2 REPRESENTATION LEARNING FOR AFFINITY PREDICTION

As a fundamental building block of ligand- and structure-based affinity prediction, machine learning models for encoding molecules and proteins have attracted a lot of attention in the research community. Based on the input data and model type, existing studies can be divided into following three categories.

Hand-crafted feature based backbones. Many early studies enlist domain experts to design features from molecules and proteins which contain rich biological and chemical knowledge, such as Morgan fingerprints (Morgan, 1965), circular fingerprints (Glen et al., 2006), and extended-connectivity fingerprint (Rogers & Hahn, 2010). Then, these hand-crafted features are fed to machine learning models to produce meaningful embeddings for downstream tasks. Typical models include logistic regression (Kleinbaum et al., 2002), random forest (Breiman, 2001), influence relevance voting (Swamidass et al., 2009), and neural networks (Ramsundar et al., 2015).

Sequence-based backbones. Since both molecules and proteins have their own sequential formats, SMILES (Weininger, 1988) and amino-acid sequence (Sanger, 1952), it is reasonable to utilize models which can naively deal with the sequential data, including 1D-CNN (Hirohara et al., 2018), RNN (Goh et al., 2017), and BERT (Wang et al., 2019a; Brandes et al., 2021). Specifically, some studies (Xu et al., 2017; Min et al., 2021) introduce self-supervised techniques from natural language processing to generate high-quality embeddings. However, 1D linearization of molecular structure highly depends on the traverse order of molecular graphs, which means that two atoms that are close in the sequence may be far apart and thus uncorrelated in the actual 2D/3D structures (e.g., the two oxygen atoms in "CC(CCCCCCO)O"), therefore hinders language models to learn effective representations that rely heavily on the relative position of tokens (Wang et al., 2021).

Graph-based backbones. To eliminate the information loss in the sequence-based models, recently, some studies start to explore the more complex graph-based representation of molecules and proteins and utilize graph neural networks (GNNs) to produce embeddings which encode the information of chemical structures, such as GIN (Xu et al., 2018), GCN (Kipf & Welling, 2016), and GAT (Velickovic et al., 2018). Other than directly applying the vanilla GNN model as the backbone, several studies try to incorporate the domain knowledge in the model design, such as ATi-FPGNN (Xiong et al., 2019), NF (Duvenaud et al., 2015), Weave (Kearnes et al., 2016), MGCN (Lu et al., 2019), MV-GNN (Ma et al., 2020), CMPNN (Song et al., 2020b), MPNN (Gilmer et al., 2017), and DMPNN (Yang et al., 2019a). Other than standard GNN models, several studies exploit Transformer-like GNN models to enhance the expressive power for training with a large number of molecules and proteins, such as GTransformer (Rong et al., 2020) and Graphormer (Ying et al., 2021).

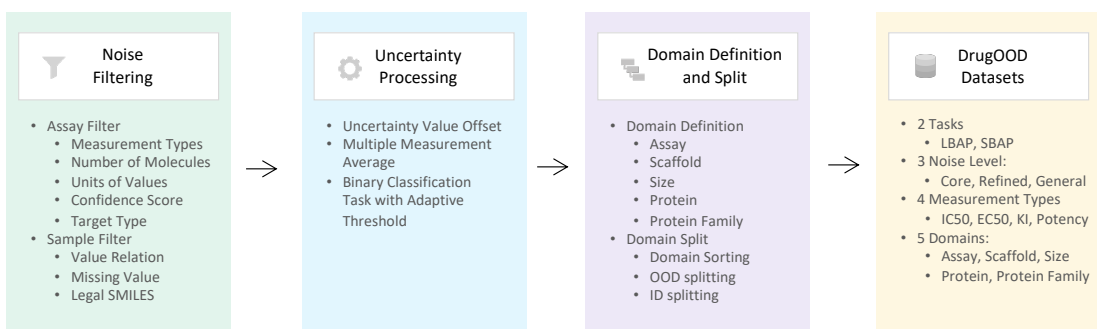


Figure 2: Overview of the automated dataset curator. We mainly implement three major steps based on the ChEMBL data source: noise filtering, uncertainty processing, and domain splitting. We have built-in 96 configuration files to generate the realized datasets with the configuration of two tasks, three noise levels, four measurement types, and five domains.

3. Automated Dataset Curator with Real-world Domain and Noise Annotations

We construct all the datasets based on ChEMBL (Mendez et al., 2019), which is a large-scale, open-access drug discovery database that aims to capture medicinal chemistry data and knowledge across the pharmaceutical research and development process. We use the latest release in the SQLite format: ChEMBL 29⁴. Moreover, we consider the setting of OOD and different noise levels, which is an inevitable problem when the machine learning model is applied to the drug development process. For example, when predicting SBAP bioactivity in practice, the target protein used in the model inference could be very different from that in the training set and even does not belong to the same protein family. The real-world domain gap will invoke challenges to the accuracy of the model. On the other hand, the data used in the wild often have various kinds of noise, e.g. activities measured through experiments often have different confidence levels and different “cut-off” noise. Therefore, it is necessary to construct data sets with varying levels of noise in order to better align with the real scenarios.

In the process of drug development, many predictive tasks are involved. Here, we consider two crucial tasks from computer aided drug discovery (Sliwoski et al., 2013): ligand based affinity prediction (LBAP) and structure based affinity prediction (SBAP). In LBAP, we follow the common practice and do not involve any protein target information, which is usually used in the activity prediction for one specific protein target. In SBAP, we consider both the target and drug information to predict the binding activity of ligands, aiming to develop models that can generalize across different protein targets.

4. Download link: http://ftp.ebi.ac.uk/pub/databases/chembl/ChEMBLdb/releases/chembl_29/chembl_29_sqlite.tar.gz

3.1 Filtering Data with Different Noise Levels

ChEMBL contains the experimental results reported in previously published papers, sorted by "assays". However, the activity values for different assays and even different molecules in the same assay may have different accuracy and confidence levels. For example, assays that record the results of high-throughput screens (HTS) usually have less accurate activity values. The data with different accuracy constitute different noise annotations. Therefore, we set up filters with different stringency to screen for datasets with varying noise levels.

Our filters consist assay filters and sample filters, which aim to screen for the required assays and samples. Specifically, we have built-in 5 assay filters and 3 sample filters in advance. The details are shown as follows.

► Assay Filter

- **Measurement Type:** Filtering out the assays with required measurement types, e.g. IC50, EC50. Due to the big difference in meaning between measurement types, and its difficulty to merge them, we generate different datasets for each measurement types.
- **Number of Molecules:** Assay noise is strongly related to the number of molecules in an assay. For example, large assays are often derived from high-throughput screens that are very noisy. Hence we set different molecules number limits for different noise levels.
- **Units of Values:** The units of activity values recorded in ChEMBL are chaotic, e.g. nM, %, None. The conversion between some units is easy, such as nM and μ M. But most of them cannot be converted between each other.
- **Confidence Score:** Due to the complex settings of different experimental assays, sometimes it is not certain that the target that interacts with the compound is our designated target. Confidence score of an assay indicating how accurately the assigned target(s) represent(s) the actually assay target.
- **Target Type:** There are dozens of target types in ChEMBL, from 'single protein' to 'organism'. Different target types have different confidence levels. For SBAP tasks, the target type of a 'single protein' is more reliable than others.

► Sample Filter

- **Value Relation:** In many cases, the precise activity values of certain molecules could not be obtained, but given a rough range. ChEMBL records qualitative values with different relationships, e.g. '=', '>', '<', '>>'. Obviously, '=' means the value is accurate, and the others means the value is not accurate.
- **Missing Value:** Filtering samples with any missing value.
- **Legal SMILES:** Filtering samples with illegal molecules.

The configurations of each filter for three different noise levels are shown in the Table 1. One can see that the three noise levels are now annotated jointly by "Confidence

Table 1: The filter configurations for three noise levels. * means the user configuration will specify the measurement type. '—' denotes no restriction. ✓ indicates the conditions need to be met. "SP": single protein. "PC": protein complex. "PF": protein family. One can see that the three noise levels are now annotated jointly by "Confidence Score", "Value Relation", "Number of Molecules" and "Target Type", which are shown in blue color.

	Name	Core	Refined	General
Assay Filter	Measurement Type	*	*	*
	Number of Molecules	[50, 3000]	[32, 5000]	[10, 5000]
	Units of Values	{ nM, uM }	{ nM, uM }	{ nM, uM }
	Confidence Score	≥ 9	≥ 3	—
Sample Filter	Target Type	{ SP }	{ SP, PC, PF }	—
	Value Relation	{ $=, \sim$ }	{ $=, \sim, \geq, \leq$ }	{ $=, \sim, \geq, \leq, >, <$ }
	Missing Value	✓	✓	✓
	Legal SMILES	✓	✓	✓

Score", "Value Relation", "Number of Molecules" and "Target Type", which are shown in blue color. In Figure 1, we display some examples of the SBAP dataset, demonstrating different kinds of noise levels.

3.2 Processing Uncertainty and Multiple Measurements

As mentioned above, ChEMBL records many activity values in an uncertainty way, and they were reported as above or below the highest or lowest concentration tested. Here, we follow the practice in pQSAR 2.0 (Martin et al., 2017) and offset them by 10-fold. Meanwhile, since the same molecule may be reported in different sources, the same molecule may also appear in multiple assays in ChEMBL. We call this phenomenon "multiple measurements". Following the common practice (Hu et al., 2020), we average all the multiple measurements. For LBAP task, we average all the activity values for the same molecule before domain split. While for SBAP task, when the molecule and target pair is the same, we average their activity values.

3.3 Binary Classification Task with Adaptive Threshold

While ChEMBL record activity values as floating numbers, benchmarking OOD tasks as regression tasks is known to be extremely hard because various noises such as uncertainty measurements. Additionally, in the process of drug development, practitioners habitually consider whether a compound is active/inactive. Therefore, using a binary classification task is more robust and good enough to make decisions in the drug development. However, in practice the threshold for binary classification depends on the specific circumstances of the drug development project. Here, we choose to use an adaptive threshold method that can adapt to a wider range of situations. In particular, the median value of all compounds in the generated dataset defines the threshold, but the range of allowed thresholds are fixed to be $4 \leq pValue \leq 6$, where $pValue = -\log_{10}(Activity Value)$. If the median is outside this range, a fixed threshold $pValue = 5$ is applied, which follows the common practice (Mayr et al., 2018; Stanley et al., 2021) in drug discovery. In this

way, we can try our best to keep the dataset balanced while making the generated tasks meaningful.

3.4 Domain Definition and Split

3.4.1 DOMAIN DEFINITION

As mentioned before, distributional shift is a common phenomenon in the drug development process. In order to make our benchmark more in line with the needs of drug discovery and development, we consider the OOD setting in the benchmark. In the process of drug research and development, when predicting the bioactivities of small molecules, we may encounter very different molecular scaffolds, sizes and so on from the model training set. These differences may also be reflected in the target in the SBAP task. Hence, for LBAP task, we consider the following three domains: assay, scaffold and molecule size. For SBAP tasks, in addition to the three domains mentioned above, we also consider two additional target-specific domains: protein and protein family. The user can also easily customize the domain through the configuration file and generate the corresponding dataset. The details of the five domains are as follows.

- **Assay:** Samples in the same assay are put into the same domain. Due to the great differences in different assay environments, the activity values measured by different assays will have a large shift. At the same time, different assays have very different types of experiments and test targets.
- **Scaffold:** Samples with the same molecular scaffold belong to the same domain. The molecular properties of different scaffolds are often quite different.
- **Size:** A domain consists of samples with the *same* number of atoms. As a result, we can test the model’s performance on molecules that are quite different.
- **Protein:** In SBAP task, samples with the same target protein are in the same domain, in order to test the model performance when meeting a never-seen-before protein target.
- **Protein Family:** In SBAP tasks, samples with targets from the same family of proteins are in the same domain. Compared with protein domains, there are much less protein family domains albeit with greater differences among each other.

3.4.2 DOMAIN SPLIT

Based on the generated domains, we need to split them into training, OOD validation and OOD testing set. Our goal is to make the domain shifts between the training set and the OOD validation/testing set as significant as possible. This leads to the question of how to measure the differences between different domains and how to sort them into the training set and validation/testing set. Here, we design a general pipeline, that is, firstly generate domain descriptor for each domain, and then sort the domains with descriptors. Then the sorted domains are sequentially divided into training set, OOD validation and testing

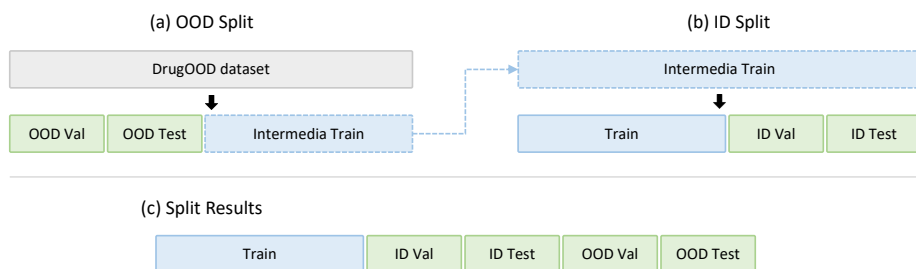


Figure 3: Illustration of our domain split process: (a) *OOD Split*: Based on the sorted data, we sequentially split them into an intermediate training set, OOD validation, and testing set. We try to keep the proportion of training, validation, and testing samples at around 6:2:2. (b) *ID Split*: From the intermediate training set, we further separate the final train, ID validation, and ID test sets. (c) We get training, ID validation, ID test, OOD validation, and OOD test sets after executing the above steps.

set (Figure 3 (a)). Meanwhile, the number of domains in different splits are controlled by the number of total samples in each splits, and the proportion of sample numbers is trying to be kept at 6:2:2 for training, validation and testing set.

In the DrugOOD framework, we have built-in two domain descriptor generation methods as follows.

- **Domain Capacity:** The domain descriptor is the number of samples in this domain. In practice, we found that the number of samples in a domain can well represent the characteristics of a domain. For example, an assay with 5000 molecules is usually different from an assay with 10 molecules in assay type. For SBAP, a protein family that contains 1000 different proteins is very likely to be different from the protein family that contains only 10 proteins. The descriptor is applied to the domains of assay, protein and protein family.
- **Molecular Size:** For the size domain, the size itself is already a good domain descriptor and can be applied to sort the domains, which we found to effectively increase the generalization gap in practice. The descriptor is applied to the domain of size and scaffold.

Generating in-distribution data subsets. After splitting the training, OOD validation and OOD test sets, we split the ID validation and ID testing sets from the resultant training set (Figure 3 (b)). We follow similar settings as of WILDS (Koh et al., 2021), the ID validation and testing sets are merged from the randomly selected samples of each domain in the training set. The ratio of the number of samples in the OOD and ID validation/test sets can be easily modified through the configuration files. After this process, we get the final training, ID validation, ID test, OOD validation, OOD test sets (Figure 3 (c)).

Table 2: Statistical information of datasets in LBAP tasks under the IC50 measurement type. *Domain*[#] represents the number of domains, and *Sample*[#] represents the number of data points.

Data subset	<i>Domain</i> [#]	<i>Sample</i> [#]
Drug00D-lbap-core-ic50-assay	1,324	95,236
Drug00D-lbap-refined-ic50-assay	5,612	266,522
Drug00D-lbap-general-ic50-assay	29,938	568,556
Drug00D-lbap-core-ic50-scaffold	34,807	95,236
Drug00D-lbap-refined-ic50-scaffold	90,888	266,522
Drug00D-lbap-general-ic50-scaffold	186,875	568,556
Drug00D-lbap-core-ic50-size	251	95,236
Drug00D-lbap-refined-ic50-size	288	266,522
Drug00D-lbap-general-ic50-size	337	568,556

3.5 Overview of the Dataset Curation Pipeline

The overview of the datasets curation pipeline is shown in Figure 2. It mainly includes four major steps: filtering data with different noise levels, processing uncertainty and multi-measurements, binary classification task with adaptive threshold and domain split. We have built-in 96 configuration files to generate different datasets with the configuration of 2 tasks, 3 noise levels, 4 measurement types, and 5 domains. With our Drug00D dataset curation, the user can easily obtain the required datasets through customizing the configuration files.

Here, we show some statistics of datasets generated by our built-in configuration files. Table 2 and Table 3 show the statistics of domains and samples in LBAP task and SBAP task under IC50 measurement type, respectively. We can see that as the number of samples increases, the noise level also increases. Meanwhile, for the same noise level, there are huge differences in the number of domains generated by different domain split methods, which will challenge the applicability of OOD algorithm in different domain numbers. In order to show the comparison of data volume under different measurement types, we count the samples of different measurement types under different noise levels, as shown in Figure 4. As we can see, the number of samples varies greatly under different measurement types in ChEMBL. Meanwhile, different measurement types may also bring different noise levels. Our curation can generate specific measurement types of datasets according to the needs of specific drug development scenarios. More statistical information of the Drug00D datasets under different setting are summarized in Table 10 and Table 11.

4. Benchmarking State-of-the-art OOD Algorithms

Our benchmark implements and evaluates algorithms from various perspectives, including *architecture design* and *domain generalization* methods, to cover a wide range of approaches to addressing the distribution shift problem. We believe this is the first paper to comprehensively evaluate a large set of approaches under various settings for the Drug00D problem.

Table 3: Statistical information of some DrugOOD datasets. *Domain[#]* represents the number of domains, and *Sample[#]* represents the number of data points.

Data subset	<i>Domain[#]</i>	<i>Sample[#]</i>
DrugOOD-sbap-core-ic50-assay	1,455	120,498
DrugOOD-sbap-refined-ic50-assay	6,409	339,930
DrugOOD-sbap-general-ic50-assay	23,868	583,401
DrugOOD-sbap-core-ic50-scaffold	34,807	120,498
DrugOOD-sbap-refined-ic50-scaffold	89,627	339,930
DrugOOD-sbap-general-ic50-scaffold	145,768	583,401
DrugOOD-sbap-core-ic50-size	251	120,498
DrugOOD-sbap-refined-ic50-size	288	339,930
DrugOOD-sbap-general-ic50-size	327	583,401
DrugOOD-sbap-core-ic50-protein	677	120,498
DrugOOD-sbap-refined-ic50-protein	1,483	339,930
DrugOOD-sbap-general-ic50-protein	2,671	583,401
DrugOOD-sbap-core-ic50-protein-family	13	120,498
DrugOOD-sbap-refined-ic50-protein-family	15	339,930
DrugOOD-sbap-general-ic50-protein-family	15	583,401

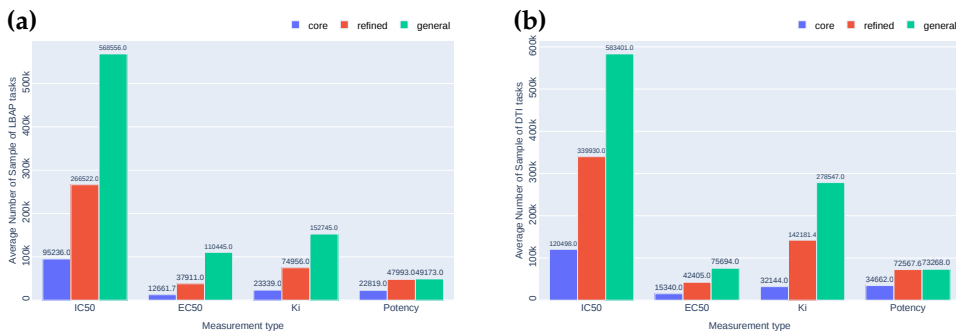


Figure 4: Statistics of samples for (a) LBAP and (b) SBAP tasks. Each column represents the average of all domain sample sizes under a certain noise level and measurement type.

4.1 Architecture Design

It’s known that the expressive power of the model is largely depend on the network architecture. How to design the network architecture for the better ability to fit the target function and robustness to the noise is a popular area of out-of-distribution data problem. Based on the DGL-LifeSci package (Li et al., 2021a), we benchmark and evaluate following graph-based backbones: GIN (Xu et al., 2018), GCN (Kipf & Welling, 2016), GAT (Velickovic et al., 2018), SchNet (Schütt et al., 2017), Weave (Kearnes et al., 2016), MGCN (Lu et al., 2019), ATi-FPGNN (Xiong et al., 2019), NF (Duvenaud et al., 2015) and GTransformer (Rong et al., 2020). For the Sequence based input, we adopt the BERT (Devlin et al., 2018) and Protein-BERT (Brandes et al., 2021) as feature extractors. The backbones are extended to regression and classification tasks by a readout function and an MLP layer.

We use a standard model structure for each type of data: GIN (Kipf & Welling, 2016) for molecular graphs and BERT (Devlin et al., 2018) for protein amino acid sequences. In addition, the other models mentioned above were also used for some of the datasets in

Table 4: The in-distribution (ID) vs out of distribution (OOD) of datasets with measurement type of IC50 trained with empirical risk minimization. The ID test datasets are drawn from the training data with the same distribution, and the OOD test data are distinct from the training data, which are described in Section 3. We adopt the Area under the ROC Curve (AUROC) to estimate model performance; the higher score is better. In all tables in this paper, we report in parentheses the standard deviation of 3 replications, which measures the variability among replications. All datasets show performance drops due to distribution shift, with substantially better ID performance than OOD performance. More experimental results under different setting are shown in Table 12 in Appendix.

Dataset	In-dist	Out-of-Dist	Gap
Drug00D-lbap-core-ic50-assay	89.62 (2.04)	71.98 (0.29)	17.64
Drug00D-lbap-core-ic50-scaffold	87.15 (0.48)	69.54 (0.52)	17.60
Drug00D-lbap-core-ic50-size	92.35 (0.15)	67.48 (0.47)	24.87
Drug00D-lbap-refined-ic50-assay	89.25 (0.64)	72.70 (0.00)	16.55
Drug00D-lbap-refined-ic50-scaffold	86.23 (0.08)	70.45 (0.54)	15.78
Drug00D-lbap-refined-ic50-size	91.31 (0.07)	68.74 (0.37)	22.58
Drug00D-lbap-general-ic50-assay	85.19 (1.15)	69.88 (0.13)	15.32
Drug00D-lbap-general-ic50-scaffold	85.15 (0.24)	67.55 (0.09)	17.60
Drug00D-lbap-general-ic50-size	89.77 (0.08)	66.05 (0.32)	23.72
Drug00D-sbap-core-ic50-protein	90.71 (0.29)	68.87 (0.53)	21.84
Drug00D-sbap-core-ic50-protein-family	89.88 (1.44)	72.20 (0.14)	17.68
Drug00D-sbap-refined-ic50-protein	86.87 (1.41)	69.51 (0.30)	17.36
Drug00D-sbap-refined-ic50-protein-family	86.44 (3.07)	70.61 (0.42)	15.82
Drug00D-sbap-general-ic50-protein	85.34 (1.67)	68.48 (0.27)	16.86
Drug00D-sbap-general-ic50-protein-family	79.18 (2.69)	68.60 (0.68)	10.58

measuring the effect of model structure on generalization ability. Following the model selection strategy in (Koh et al., 2021), we use a distinct OOD validation set for model early stopping and hyper-parameter tuning. The OOD validation set is drawn from a similar distribution of the training set, which distant from the OOD test set. For example, in the assay-based datasets, the training, validation, testing each consists of molecules from distinct sets of the assay environment. We detail the experimental protocol in Section 6.

Table 4 shows that for each dataset with the measurement type of IC50, the OOD performance is always significantly lower than the performance of the corresponding ID setting.

4.2 Domain Generalization Algorithms

In machine learning, models are commonly optimized by the empirical risk minimization (ERM), which trains the model to minimize the average training loss. To improve the model robustness under the distribution shift, current methods tend to learn invariant representations that can generalize across domains. There are two main directions: domain alignment and invariant predictors. Common approaches to domain alignment is to minimize the divergence of feature distributions from different domains across distance metrics, such as maximum mean discrepancy (Tzeng et al., 2014; Long et al., 2015) and adversarial loss (Ganin et al., 2016; Li et al., 2018), Wasserstein distance (Zhou et al., 2020a). In addition, other conventional methods along this line of research are adopting data augmentation. For example, Mixup (Zhang et al., 2017) augmentation proposes to

Table 5: The out-of-distribution (OOD) performance of baseline models trained with different OOD algorithms on the DrugOOD-lbap-ic50 dataset.

Algorithms	Assay			Scaffold			Size		
	core	refined	general	core	refined	general	core	refined	general
ERM	71.98 (0.29)	69.54 (0.52)	67.48 (0.47)	69.88 (0.13)	67.55 (0.09)	66.05 (0.32)	72.70 (0.00)	70.45 (0.54)	68.74 (0.37)
IRM	69.22 (0.51)	64.94 (0.30)	57.00 (0.39)	69.21 (0.16)	63.78 (0.53)	60.52 (0.35)	71.68 (0.53)	67.97 (0.66)	59.99 (0.48)
DeepCoral	71.76 (0.60)	68.54 (0.01)	57.31 (0.44)	69.47 (0.13)	64.84 (0.53)	61.09 (0.23)	71.45 (0.09)	69.35 (0.73)	62.01 (0.38)
DANN	70.08 (0.65)	66.37 (0.20)	63.45 (0.18)	65.12 (0.94)	62.90 (1.02)	64.74 (0.27)	67.20 (0.68)	67.26 (0.95)	66.83 (0.08)
Mixup	71.34 (0.41)	69.29 (0.24)	67.73 (0.27)	69.87 (0.17)	67.64 (0.16)	66.01 (0.14)	72.13 (0.21)	70.68 (0.16)	68.69 (0.13)
GroupDro	71.54 (0.46)	66.67 (0.67)	60.90 (1.23)	69.36 (0.09)	64.91 (0.25)	61.41 (0.10)	71.40 (0.52)	69.08 (0.38)	62.15 (0.54)

construct additional virtual training data by convex combination of both samples and labels from the original datasets. Follow-up works applied a similar idea to generate more domain and enhance consistency of features during training (Yue et al., 2019; Zhou et al., 2020b; Xu et al., 2020; Yan et al., 2020b; Shu et al., 2021; Wang et al., 2020; Yao et al., 2022), or synthesize unseen domain in an adversarial way to imitate the challenging test domains (Zhao et al., 2020; Qiao et al., 2020; Volpi et al., 2018).

For learning invariant predictors, the core idea is to enhance the correlations between the invariant representation and the labels. Representatively, invariant risk minimization (IRM) (Arjovsky et al., 2019) penalizes the feature representation of each domain that has a different optimal linear classifier, intending to find a predictor that performs well in all domains. Following up IRM, subsequent approaches propose powerful regularizers by penalizing variance of risk across domains (Krueger et al., 2021a), by adjusting gradients across domains (Koyama & Yamaguchi, 2020), by smoothing interpolation paths across domains (Chuang & Mroueh, 2021). An alternative to IRM is to combat spurious domain correlation, a core challenge for the sub-population shift problem (Koh et al., 2021), by directly optimizing the worst-group performance with Distributionally Robust Optimization (Sagawa et al., 2019; Zhang et al., 2020; Zhou et al., 2021a), generating additional samples around the minority groups (Goel et al., 2020), and re-weighting among groups with various size (Sagawa et al., 2020), or additional regulations (Chang et al., 2020).

We implement and evaluate the following representative OOD methods:

- **ERM:** ERM optimizes the model by minimizing the average empirical loss on observed training data.
- **IRM:** IRM penalizes feature distributions for domains that have different optimum predictors.
- **DeepCoral:** DeepCoral penalizes differences in the means and covariances of the feature distributions (i.e., the distribution of last layer activations in a neural network) for each domain. Conceptually, DeepCoral is similar to other methods that encourage feature representations to have the same distribution across domains.
- **DANN:** Like IRM and DeepCoral, DANN encourages feature representations to be consistent across domains.

- **Mixup:** Mixup constructs additional virtual training examples from two examples drawn at random from the training data, which alleviates the effects of domain-related spurious information through data interpolation.
- **GroupDro:** GroupDro uses distributionally robust optimization methods to minimize worst-case losses, aiming to combat spurious correlations explicitly.

Table 5 summarizes the experimental results on the datasets with IC50 measurement type, showing that latest OOD algorithms exhibit *no clear improvement* over the simple ERM algorithm. There may be several reasons for this: 1). the molecular graph data are different from visual and textual input by nature, thus making it challenging to use conventional strategies directly; 2). these algorithms are usually designed for datasets that contain enough data per domain, so it is difficult to apply directly to datasets that have a large number of domains but few samples per domain. There is a need for improved approaches to realistic DrugOOD problems, based on the results. Additionally, current OOD research focus almost exclusively on the single-instance prediction tasks while overlook multi-instance prediction tasks, and how to better handle the distribution shift in multiple instance domains (e.g., molecule and protein inputs in the SBAP task) remains an open problem. Lastly, while not explored in this paper, the large-scale realistic datasets always come with non-negligible inherent noise, both aleatoric and epistemic (Lazic & Williams, 2021). And how to incorporate noise learning with OOD generalization to boost model’s robustness and generalization in the meantime is an important research direction.

5. Implementations and Package Usage

DrugOOD develops a comprehensive benchmark for developing and evaluating OOD generalization algorithms. Different with other codebases, DrugOOD builds on the OpenMMLab project (Chen et al., 2019), owning the following features:

Customizable dataset. DrugOOD supports various formats of data, providing related processing and converting tools. We provide 96 realized sub-datasets in advance. In addition to this, users can additionally specify additional conditions to easily customize new datasets from the original source dataset.

Modular design. Building on the design of OpenMMLab projects, we decompose the framework into different components and one can easily construct new OOD algorithms by combing these modules.

Support for multiple frameworks out of the box. DrugOOD codebase directly supports various popular and contemporary OOD generalization algorithms, e.g. DeepCoral, IRM, DANN, Mixup etc.

With the above abstraction, our benchmark framework is illustrated in Figure 5. By simply creating some new components and assembling existing ones, the researchers can develop their approach efficiently.

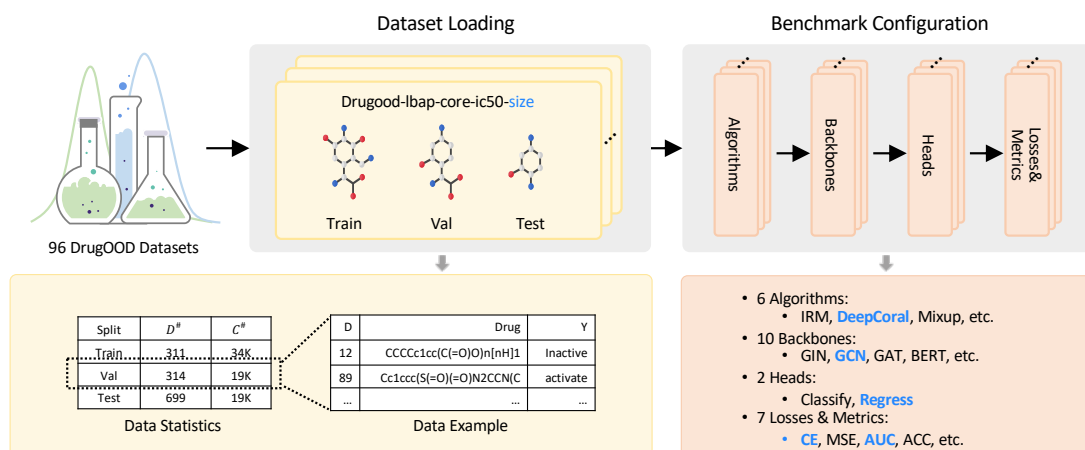


Figure 5: Overview of the DrugOOD benchmark. DrugOOD conducts a comprehensive benchmark for developing and evaluating OOD generalization algorithms for AIDD. After loading any of the datasets generated by the data curator, users can flexibly combine different types of modules, including algorithms, backbones, etc., to develop OOD generalization algorithms in a flexible and disciplined manner.

5.1 Dataset Curation

The DrugOOD package provides a simple, standardized dataset curator based on the large-scale bioassay deposition website ChEMBL (Mendez et al., 2019), by providing a modified curation files, the researcher can easily re-configure the curation process. Specifically, we have provided 96 built-in configuration files for generating OOD dataset spanning various domains, noise annotations and measurement types. The Listing 1 provides a simple example, which covers all of the steps of generating an OOD dataset from ChEMBL.

```

1 # configure curation pipeline
2 curator = dict(
3     task="lbap",
4     chembl='./chembl_29_sqlite/chembl_29.db',
5     save_dir=".data/lbap/lbap_core_EC50_assay",
6     # noise filtering
7     filter=dict(
8         assay_filter=dict(
9             measurement_type=["EC50"],
10            assay_value_units=["nM", "uM"],
11            molecules_number=[50, 3000],
12            confidence_score=9
13        ),
14        sample_filter=dict(
15            filter_none=True,
16            smile_exist=True,
17            smile_legal=True,
18            value_relation=["=", "~"]
19        )
20    ),
21    # uncertainty filtering

```

```

22     uncertainty=dict(
23         multiple_measurement_average=True,
24         uncertainty_delta={'<': -1, '<=': -1, '>': 1, '>=': 1},
25         binary_threshold=dict(
26             lower_bound=4,
27             upper_bound=6,
28             fix_value=5)
29     ),
30     # domain split
31     split=dict(
32         domain=dict(
33             domain_generate_field="assay_id",
34             domain_name="assay",
35             sort_func="domain_capacity"
36         ),
37
38         fractions=dict(
39             train_fraction_ood=0.6,
40             val_fraction_ood=0.2,
41             IID_train_sample_fractions=0.6,
42             IID_val_sample_fractions=0.2
43         )
44     ),
45 )
46 )

```

Code Listing 1: Dataset curation example

5.2 Dataset Loading

As shown in Listing 2, DrugOOD provides a flexible and uniform interface for building data pipelines, allowing users to easily and quickly adjust the experimental data flow. Meanwhile, Standardized and automated evaluation of specified dataset partitions can be easily implemented by a few lines of code.

```

1 dataset_type = 'MOL'
2 subset = 'lbap_ic50_core_assay'
3 data_prefix = "data/drugood"
4 # data preprocess pipeline
5 pipeline = [
6     dict(type="SmileToGraph", keys=['input']),
7     dict(type='ToTensor', keys=['gt_label']),
8     dict(type='Collect', keys=['input', 'gt_label', 'meta'])
9 ]
10 # data sampling strategy
11 sample_config = dict(
12     uniform_over_groups=None,
13     n_groups_per_batch=2,
14     distinct_groups=True
15 )
16 # data loading schedule
17 data = dict(
18     samples_per_gpu=256,

```

```

19 workers_per_gpu=0,
20 train=dict(
21     split="train",
22     type=dataset_type,
23     subset=subset,
24     data_prefix=data_prefix,
25     pipeline=pipeline,
26     sample_mode="group",
27     sample_config=sample_config
28 ),
29 val=dict(
30     split="val",
31     type=dataset_type,
32     subset=subset,
33     data_prefix=data_prefix,
34     pipeline=pipeline,
35     rule="greater", # model selection
36     save_best="auc"
37 ),
38 test=dict(
39     split="test",
40     type=dataset_type,
41     subset=subset,
42     data_prefix=data_prefix,
43     pipeline=pipeline)
44 )

```

Code Listing 2: Dataset loading example

5.3 Algorithm Configuration

DrugOOD also supports popular and contemporary OOD generalization algorithm out of box. Users can easily configure different modules to construct and develop new OOD generalization algorithms effectively. We provide an example of building algorithm in few lines code, as shown in Listing 3.

```

1 # algorithm configuration
2 model = dict(
3     type="ERM",
4     # backbone
5     tasker=dict(
6         type='Classifier',
7         backbone=dict(
8             type='GIN', # backbone setting
9             num_node_emb_list=[39],
10            num_edge_emb_list=[10],
11            emb_dim=256,
12            dropout=0.0,
13        ),
14        head=dict(
15            type='LinearClsHead',
16            num_classes=2,
17            in_channels=256,

```

```
18     loss=dict(type='CrossEntropyLoss'))
19 ))
```

Code Listing 3: Algorithm configuration example

6. Empirical Studies

We present typical experimental results and corresponding analysis in this section. More results and details are deferred to the Appendix.

6.1 Ligand Based Affinity Prediction (LBAP)

Precisely predicting the affinity score of small molecules will greatly boost the process of drug discovery by reducing the needs of costly laboratory experiments. However, the experimental data available for training such models is limited compared to the extremely diverse and combinatorially large universe of candidate molecules that we would want to make predictions on. In this paper, we study the domain variation in experimental assay, molecules sizes, molecule sizes between training and test molecules.

6.1.1 SETUP

Problem Definition. For the task of LBAP, we study a domain generalization problem where model needs to be generalized to the molecules from different domain splits. Aligned with the knowledge of biochemistry, we define the following three domains: assay, scaffold and molecular size. As an illustration, we treat the LBAP problem as a binary classification problem, where the input x is the graph data of a small molecule, label y is the ground truth (active or inactive) of binary affinity classification, and the d represents domain identifier for one specific domain splits.

Data Info. As mentioned before, we preprocess the ChEMBL dataset and generate in total 36 exemplar datasets with varying noise levels, measurements types, and domain definitions. Each small molecule in each dataset is represented as a graph, where the nodes are atoms and edges are chemical bonds. Following the pre-processing strategy in (Xiong et al., 2019), we preprocess the molecules via the RDKit package (Landrum, 2013). Input node features are 39-dimensional vectors including atomic symbol, hybridization, hydrogens and so on. Input edge features are 10-dimensional vectors including bond type, conjugation, ring and bond stereo chemistry. Following the detailed splitting strategy in Figure 3 of Section 3.4, we split the dataset via three types of domain annotations:

- **Assay:** Samples in the same assay are divided into the same domain. Due to the big differences of experimental environments and protein targets in various assays, the bioactivity values measured by those assays will have a large shift. In this setting, we split the dataset along assays. This split provides a realistic estimate of model performance in prospective experimental settings by separating different molecules into different experimental environments. We assign the assays that contain large number of samples to the training set, and the assays with small number of samples

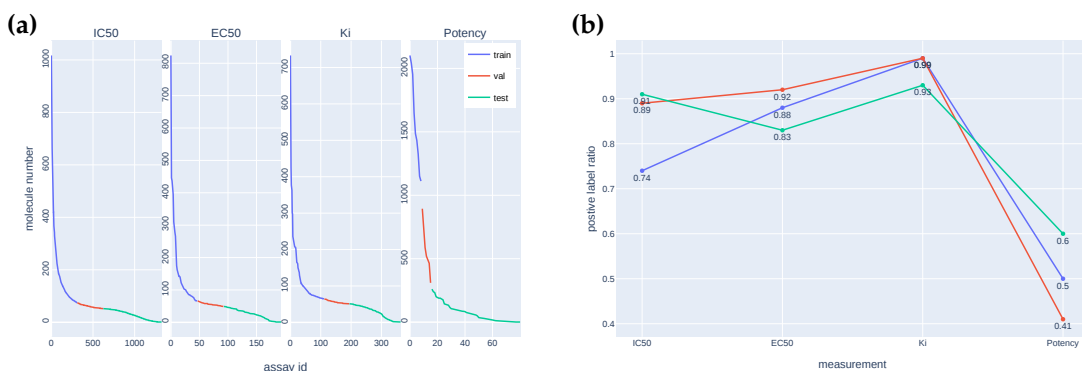


Figure 6: Analysis of the assay domain in the realized Drug00D dataset. (a) shows the distribution of molecule numbers in the assay environment for different measurement types (left to right: IC50, EC50, Ki and Potency) and (b) shows the ratio of positive samples of four measurement types in the train/validation/test splits. Note that here the train, val, test refer to the Intermediate Train, OOD val and OOD test datasets in Figure 3.

to the test set. After such an assignment, the domain shifts between the training set and the OOD validation/testing set become sufficiently large. The proportion of samples is kept at around 6:2:2 in training, validation, test set.

Here takes the Drug00D-lbap-core-ic50-assay dataset as an illustration here.

- **Train:** Contain total 34,179 molecules from the largest 311 assays with an average of 110 molecules per assay.
- **Validation (ID):** Contain total 11314 molecules from the same 311 assays as in the training sets.
- **Test (ID):** Contain total 11,683 molecules from the same 311 assay environments as in the training sets.
- **Validation (OOD):** Contain total 19,028 molecules from the next largest 314 assays with an average of 60.6 molecules per assay.
- **Test (OOD):** Contain total 19,302 molecules from the smallest 314 assays with an average of 27.6 molecules per assay.

Figure 6 illustrates the analysis of the assay domain in the realized Drug00D dataset. As shown in Figure 6 (a), the statistics of the assays in terms of the numbers of molecules in each assay, which implies that the scale of the experiments is highly skewed, with the test set containing the assay with the fewest molecules. However, the difference in assay environments does not significantly change the statistics of the learning target in each split. In Figure 6, the label statistics still remain very similar in the training/validation/test splits, indicating that the main distribution variation comes from differences in the detection environment.

- **Scaffold:** Scaffold split has been widely used in previous benchmarks (Koh et al., 2021; Hu et al., 2020), which splits datasets based on scaffold structure. Similarly,

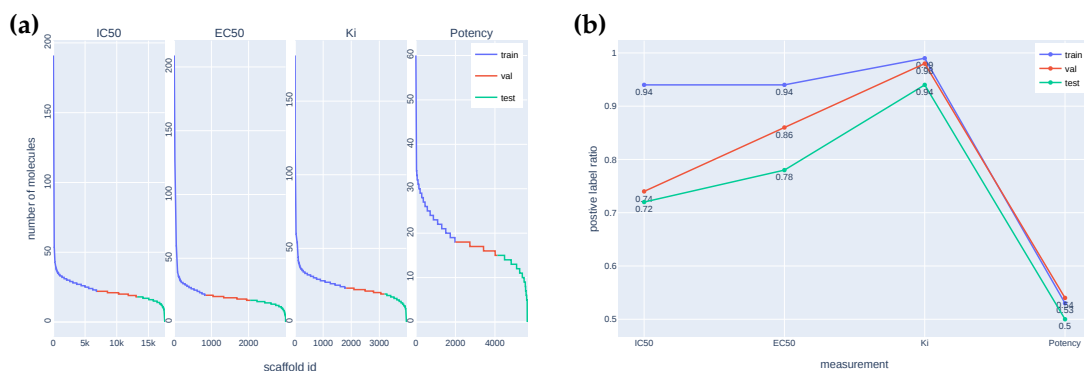


Figure 7: Analysis of the scaffold domain in the DrugOOD dataset. (a) shows the distribution of number of molecules wrt the scaffold id and (b) shows the positive ratio of molecules of four measurement types in the train/validation/test splits. Note that here the train, val, test refer to the Intermediate Train, OOD val and OOD test datasets in Figure 3.

we assign the largest scaffolds to training set and smallest scaffolds to the test set to ensure its maximal diversity in scaffold structure. Take the DrugOOD-lbap-core-ic50-scaffold dataset as examples, the detailed information of splits are:

- **Train:** Contain in total 21,519 molecules from the largest 6,881 scaffolds with an average of 3.12 molecules per scaffold.
- **Validation (ID):** Contain in total 4,920 molecules from the 1,912 scaffolds with an average of 2.57 molecules per scaffold.
- **Test (ID):** Have 24,112 scaffolds, with in total 30,708 molecules.
- **Validation (OOD):** The next largest 6,345 scaffolds, with in total 11,683 molecules, and an average of 1.84 molecules per scaffold.
- **Test (OOD):** The smallest 4,350 scaffolds, with in total 19,048 molecules, and an average of 4.42 molecules per scaffold.

In the same way, we plot the statics of the scaffolds in terms of the size of each scaffold. As shown in Figure 7, we again observe that the distribution is highly skewed and the test partition contains the smallest scaffolds.

- **Size:** We put samples with the same atomic number into a domain, and separate molecules with different atomic sizes into different subsets for simulating the realistic distribution shift. We organize the molecules with the largest atomic sizes into the training set and those with smaller atomic sizes are assigned to the test set to ensure sufficient variability of atomic sizes between the training and test data. Taking the DrugOOD-lbap-core-ic50-size dataset as an example, the details of the split are as follows:

- **Train:** The largest 190 size groups, with overall 36,597 molecules, and an average of 192.61 molecules per group.

Table 6: Results of the ERM baseline on datasets: Drug00D-lbap-core-ic50-assay (first row), Drug00D-lbap-core-ic50-scaffold (second row) and Drug00D-lbap-core-ic50-size (third row). In-distribution (ID) results correspond to the train-to-train setting. Parentheses show standard deviation across 3 replicates.

Domain	Val (ID)		Val (OOD)		Test (ID)		Test (OOD)	
	ACC	AUC	ACC	AUC	ACC	AUC	ACC	AUC
Assay	89.05(0.35)	89.91(1.78)	88.79(2.23)	70.32(0.8)	89.34(0.38)	89.62(2.04)	82.14(0.86)	71.98(0.29)
Scaffold	97.04(0.13)	94.84(0.6)	85.11(0.4)	78.96(0.67)	90.51(0.14)	87.15(0.48)	76.33(0.64)	69.54(0.52)
Size	93.99(0.04)	92.91(0.16)	84.22(0.22)	81.5(0.19)	93.75(0.06)	92.35(0.15)	71.46(0.67)	67.48(0.47)

- **Validation (ID):** The 140 size groups with in total 12,153 molecules, and an average of 86.80 molecules per group.
- **Test (ID):** The other 229 groups in the intermediate training data, with total 12411 molecules.
- **Validation (OOD):** The next largest 4 size groups in addition to id data, with in total 17,660 molecules, and an average of 4,415 molecules per group.
- **Test (OOD):** The smallest 18 size groups, with in total 19,048 molecules, and an average of 1,058.22 molecules per group.

Evaluation. We evaluate models’ performance by the area under the receiver operating characteristic (AUROC), which indicates the ability of a classifier to distinguish between classes (e.g., inactive or active). The higher the AUC, the better the performance of the model at distinguishing between the positive and negative classes. Meanwhile, we also provide the results of accuracy metric.

6.1.2 BASELINE RESULTS

Model. We train the GIN model as the baseline model on each dataset from scratch with a learning rate at $1e-4$, a batch size at 256 samples and without L2-regularization. Each small molecules are pre-processed by the RDKit package to generate 39-dimensional node features and 9-dimensional edge features as input. To avoid performance degradation caused by inappropriate hyper-parameters, following the strategy in WILDS (Koh et al., 2021), we did a grid search strategy over learning rates $\{0.00003, 0.0001, 0.0005, 0.001, 0.01\}$, batch size $\{64, 128, 256, 512, 1024\}$. We report averaged results aggregated over 3 random seeds.

ERM results and performance drops. As shown in Table 4 and Table 6, model performance dropped significantly going from the train-to-train in-distribution (ID) setting to the official out-of-distribution (OOD) setting. For the assay domain, ERM achieves an average AUC score of 89.91% on the ID validation set and 89.62% on the ID test set, but only 70.32% on the OOD val set, 71.98% on the OOD test set. Similarly, for the scaffold and size domain, ERM obtains 87.15%, 92.35% AUC score on ID test set but 69.54%, 67.48% on OOD test set, respectively. The test performance of ERM drops by 17.64%, 17.60%, 24.97% points AUC score when the assay, scaffold, size split is used, respectively, suggesting that these splits are indeed harder than conventional random split, and can be used to estimate the realistic ID-OOD gap in the task of ligand based affinity prediction.

Table 7: Baseline results on three datasets for the six OOD algorithm. Drug00D-lbap-core-ic50-assay (first row), Drug00D-lbap-core-ic50-scaffold (second row) and Drug00D-lbap-core-ic50-size (third row). In-distribution (ID) results correspond to the train-to-train setting. Parentheses show standard deviation across 3 replicates.

Domain	Algos	Val (ID)		Val (OOD)		Test (ID)		Test (OOD)	
		ACC	AUC	ACC	AUC	ACC	AUC	ACC	AUC
Assay	ERM	89.05 (0.35)	89.91 (1.78)	88.79 (2.23)	70.32 (0.80)	89.34 (0.38)	89.62 (2.04)	82.14 (0.86)	71.98 (0.29)
	IRM	88.14 (0.17)	82.82 (0.87)	90.67 (0.07)	68.23 (0.31)	88.39 (0.25)	83.10 (0.46)	82.41 (0.20)	69.22 (0.51)
	DeepCoral	88.59 (0.10)	88.10 (1.42)	91.09 (0.15)	70.26 (1.04)	88.88 (0.15)	88.23 (1.42)	83.04 (0.08)	71.76 (0.60)
	DANN	88.47 (0.20)	83.39 (1.15)	91.32 (0.38)	68.30 (0.22)	88.72 (0.16)	83.20 (1.28)	83.22 (0.10)	70.08 (0.65)
	Mixup	88.80 (0.52)	89.01 (2.06)	88.76 (1.92)	69.14 (0.56)	89.01 (0.43)	88.95 (2.17)	81.65 (1.06)	71.34 (0.41)
	GroupDro	88.80 (0.15)	89.42 (0.43)	89.81 (0.41)	70.34 (0.91)	88.96 (0.15)	89.24 (0.82)	82.62 (0.23)	71.54 (0.46)
Scaffold	ERM	97.04 (0.13)	94.84 (0.60)	85.11 (0.40)	78.96 (0.67)	90.51 (0.14)	87.15 (0.48)	76.33 (0.64)	69.54 (0.52)
	IRM	92.51 (4.34)	77.66 (0.79)	81.52 (4.25)	72.77 (0.66)	86.99 (3.93)	77.22 (0.32)	72.96 (4.32)	64.94 (0.30)
	DeepCoral	95.76 (0.29)	81.60 (1.45)	85.37 (0.47)	77.09 (0.26)	89.96 (0.08)	81.13 (0.49)	76.90 (0.37)	68.54 (0.01)
	DANN	95.89 (0.09)	77.09 (0.64)	85.13 (0.81)	75.04 (0.65)	89.86 (0.10)	77.30 (0.65)	77.11 (0.66)	66.37 (0.20)
	Mixup	97.19 (0.08)	95.51 (0.44)	85.55 (0.08)	79.42 (0.62)	90.74 (0.11)	87.35 (0.33)	77.18 (0.19)	69.29 (0.24)
	GroupDro	96.02 (0.12)	78.67 (2.75)	85.01 (0.64)	74.57 (0.60)	89.87 (0.18)	78.32 (1.09)	76.18 (0.86)	66.67 (0.67)
Size	ERM	93.99 (0.04)	92.91 (0.16)	84.22 (0.22)	81.50 (0.19)	93.75 (0.06)	92.35 (0.15)	71.46 (0.67)	67.48 (0.47)
	IRM	86.77 (4.05)	66.41 (1.79)	76.49 (4.36)	60.59 (0.29)	87.08 (3.72)	69.80 (1.74)	66.39 (3.92)	57.00 (0.39)
	DeepCoral	92.40 (0.06)	70.70 (1.68)	83.34 (0.27)	61.90 (0.39)	92.28 (0.20)	73.08 (0.98)	72.36 (0.32)	57.31 (0.44)
	DANN	91.31 (2.12)	80.13 (3.59)	81.99 (2.46)	73.73 (0.49)	91.12 (2.12)	78.53 (3.71)	70.08 (3.50)	63.45 (0.18)
	Mixup	94.23 (0.21)	92.89 (0.30)	84.64 (0.26)	81.79 (0.20)	93.88 (0.17)	92.48 (0.55)	72.73 (0.68)	67.73 (0.27)
	GroupDro	92.73 (0.17)	78.46 (0.91)	83.54 (0.52)	67.68 (0.42)	92.67 (0.27)	80.02 (0.44)	72.64 (0.33)	60.90 (1.23)

More experimental results on different Drug00D lbap datasets are shown in Table 12 of the Appendix.

Results of other baselines. Table 7 shows the performance of other conventional generalization algorithms. For a fair comparison, all algorithms adopt the same backbone network. Besides, we also make additional grid searches on algorithms’ specific hyperparameters separately, IRM’s penalty weight in $\{1, 10, 100, 1000\}$ and penalty anneal iteration in $\{100, 500, 1000\}$. DeepCoral’s penalty weight in $\{0.1, 1, 10\}$, GroupDro’s step size in $\{0.001, 0.01, 0.1\}$, DANN’s inverse factor between $\{0.0001, 1\}$ and Mixup’s probability and interpolate strength between $\{0.0001, 1\}$.

As shown in Table 7, ERM almost performs better than DeepCoral, IRM, and Group DRO, all of which use assay, scaffolds, size as the domains, indicating these existing methods can not solve the Drug00D problem. Moreover, similar to the findings in the WILDS benchmark, current existing methods make model hard to fit the training data, For instance, under the scaffold domain split, DeepCoral, IRM achieves 81.6%, 77.66% AUC score in the In-Distribution validation set, respectively, while the AUC score of ERM baseline is 94.84%. Also, these methods are primarily designed for the case when each group contains a decent number of examples, which is not the common case for the drug development scenario. Finally, the SOTA OOD algorithm does not work well in the Drug00D setting, suggesting that robust methods need to be developed to solve the OOD problem for graph data.

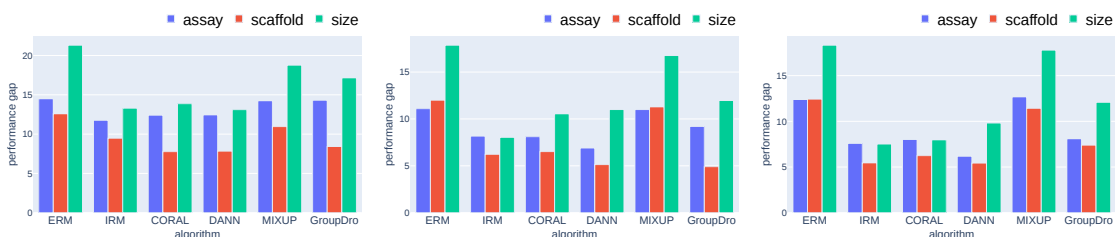


Figure 8: Performance gap on AUC of different domain splits with varying levels of noise and OOD algorithms on the DrugOOD-lbap datasets. The gap values are calculated on the OOD test set and averaged over four measurement types. From left to right: core noise level, refined noise level, general noise level. Color indicates domain annotations for LBAP tasks.

6.1.3 PERFORMANCE DROPS OF DIFFERENT DOMAINS

For the LBAP task, three types of domains are defined, and we study the performance of the model under these different domain splits. Figure 8 shows the performance degradation for different domain partitions, the gap values are computed on the test set and averaged over all measurement types. From the figure, we can conclude the following. 1) Among several divisions, the size domain brings the largest performance degradation, which is consistent with daily experimental findings, where molecules of different sizes often have very different properties. 2) As the noise level of the data set increases, the performance degradation of different domains is somewhat mitigated, and the increased data to some extent increase the generalization ability of the model. In addition, the degradation of the model performance is not further mitigated as the data continues to increase, indicating that the increase in the amount of data brings limited improvement and that a truly effective method needs to be developed to address the DrugOOD problem.

6.1.4 PERFORMANCE DROPS OF DIFFERENT NOISE LEVELS

We also investigated the ID and OOD performance at different noise levels. As shown in Table 8, we summarize different algorithms' ID and OD performance under three noise levels. From the table, one can observe that: 1) In the presence of more noise, the introduced noise produces pollution, which progressively affects the network's performance. 2) The increasing noise level brings more data, which provides more information about the dataset. From the core to refined level, we can see a narrowing of the gap between ID and OOD, however, the improvement from the refined level to general level reaches a bottleneck without significant improvement. 3) By combining the above two points, we can see that the introduction of large amounts of data with noise affects the learning of the model to a certain degree and affects its performance, but these noisy data, in turn, provide additional information so that the model is able to improve a small amount of generalization ability.

Table 8: Baseline results on datasets: Drug00D-lbap-core-ic50-assay (first row), Drug00D-lbap-refined-ic50-assay (second row) and Drug00D-lbap-general-ic50-size (third row) dataset. In-distribution (ID) results correspond to the train-to-train setting. Parentheses show standard deviation across 3 replicates.

Noise	Algos	Val (ID)		Val (OOD)		Test (ID)		Test (OOD)	
		ACC	AUC	ACC	AUC	ACC	AUC	ACC	AUC
Core	ERM	89.05 (0.35)	89.91 (1.78)	88.79 (2.23)	70.32 (0.80)	89.34 (0.38)	89.62 (2.04)	82.14 (0.86)	71.98 (0.29)
	IRM	88.14 (0.17)	82.82 (0.87)	90.67 (0.07)	68.23 (0.31)	88.39 (0.25)	83.10 (0.46)	82.41 (0.20)	69.22 (0.51)
	DeepCoral	88.59 (0.10)	88.10 (1.42)	91.09 (0.15)	70.26 (1.04)	88.88 (0.15)	88.23 (1.42)	83.04 (0.08)	71.76 (0.60)
	DANN	88.47 (0.20)	83.39 (1.15)	91.32 (0.38)	68.30 (0.22)	88.72 (0.16)	83.20 (1.28)	83.22 (0.10)	70.08 (0.65)
	Mixup	88.80 (0.52)	89.01 (2.06)	88.76 (1.92)	69.14 (0.56)	89.01 (0.43)	88.95 (2.17)	81.65 (1.06)	71.34 (0.41)
	GroupDro	88.80 (0.15)	89.42 (0.43)	89.81 (0.41)	70.34 (0.91)	88.96 (0.15)	89.24 (0.82)	82.62 (0.23)	71.54 (0.46)
Refined	ERM	91.66 (0.11)	89.06 (0.63)	91.61 (0.52)	75.57 (0.16)	91.68 (0.08)	89.25 (0.64)	84.85 (0.33)	72.70 (0.00)
	IRM	91.36 (0.08)	84.67 (0.91)	92.24 (0.13)	75.39 (0.32)	91.47 (0.08)	84.80 (0.95)	85.17 (0.23)	71.68 (0.53)
	DeepCoral	91.40 (0.05)	84.63 (0.85)	92.21 (0.23)	75.72 (0.47)	91.43 (0.04)	84.55 (0.84)	85.23 (0.13)	71.45 (0.09)
	DANN	91.21 (0.12)	78.34 (0.20)	92.27 (0.31)	72.12 (0.39)	91.33 (0.16)	78.40 (0.24)	85.09 (0.34)	67.20 (0.68)
	Mixup	91.47 (0.03)	87.30 (0.63)	92.25 (0.02)	75.67 (0.22)	91.57 (0.03)	87.36 (0.61)	85.16 (0.11)	72.13 (0.21)
	GroupDro	91.33 (0.10)	84.39 (1.72)	92.15 (0.28)	75.28 (0.23)	91.46 (0.15)	84.55 (2.20)	85.20 (0.32)	71.40 (0.52)
General	ERM	88.91 (0.14)	85.17 (1.19)	82.48 (0.07)	74.04 (0.01)	89.21 (0.13)	85.19 (1.15)	71.85 (0.08)	69.88 (0.13)
	IRM	88.37 (0.05)	80.77 (0.11)	82.37 (0.08)	73.11 (0.10)	88.67 (0.04)	80.75 (0.03)	71.51 (0.07)	69.21 (0.16)
	DeepCoral	88.41 (0.10)	81.01 (0.75)	82.43 (0.12)	73.57 (0.25)	88.71 (0.13)	81.00 (0.83)	71.65 (0.08)	69.47 (0.13)
	DANN	87.77 (0.40)	76.47 (0.71)	81.87 (0.53)	70.40 (0.57)	88.08 (0.38)	75.82 (0.57)	70.73 (0.54)	65.12 (0.94)
	Mixup	89.11 (0.31)	86.00 (1.15)	82.22 (0.28)	74.17 (0.02)	89.47 (0.23)	85.95 (1.19)	71.74 (0.07)	69.87 (0.17)
	GroupDro	88.35 (0.17)	81.06 (0.39)	82.39 (0.17)	73.45 (0.33)	88.68 (0.17)	81.31 (0.34)	71.55 (0.06)	69.36 (0.09)

6.2 Structure Based Affinity Prediction (SBAP)

6.2.1 SETUP

Compared with the LBAP task, the SBAP task considers target protein information. In our benchmark, we represent proteins as protein sequences cause the ChEMBL database only provide protein sequence information. However, Drug00D can be easily extended by incorporating 3D structure information of targets by referring to protein structure depositing database, such as PDB and uniprot (Consortium, 2014). This will be left as important future work.

6.2.2 MODEL

We use a general SBAP prediction network that extracts molecular and protein features separately, which are then concatenated together and fed into a fully connected layer to predict interaction probabilities. For the feature extraction of small molecules, we follow the setting of LBAP task and use the same network and hyperparameters. For protein sequence, we use the pre-train BERT (Devlin et al., 2018): ‘bert-base-uncased’ to extract a 768 dimensional protein feature. Then, the features of molecules and protein are concatenated and fed into a one-layer fully connected layer to predict the interaction probabilities.

6.2.3 BASELINE RESULTS

The results of different algorithms on sub-datasets with IC50 as measurement type and protein as domain are shown in Table 9. From the table, we can see that: 1) The perfor-

Table 9: Baseline results on datasets: Drug00D-sbap-core-ic50-protein (first row), Drug00D-sbap-refined-ic50-protein (second row) and Drug00D-sbap-general-ic50-protein (third row) dataset. In-distribution (ID) results correspond to the train-to-train setting. Parentheses show standard deviation across three replicates.

Noise	Algos	ID_VAL		OOD_VAL		ID_TEST		OOD_TEST	
		ACC	AUC	ACC	AUC	ACC	AUC	ACC	AUC
Core	ERM	89.28 (0.28)	90.83 (0.48)	84.22 (1.13)	74.12 (0.41)	89.32 (0.19)	90.71 (0.29)	80.37 (1.32)	68.87 (0.53)
	IRM	88.94 (0.67)	88.93 (4.03)	82.61 (2.21)	74.10 (0.39)	89.04 (0.60)	88.81 (4.03)	77.92 (4.25)	66.31 (0.45)
	DeepCoral	89.03 (0.62)	90.86 (0.95)	82.11 (1.97)	74.12 (0.46)	89.17 (0.76)	90.65 (0.97)	78.29 (2.39)	67.56 (1.01)
	DANN	88.23 (0.01)	84.58 (0.34)	84.93 (0.26)	71.47 (0.47)	88.54 (0.10)	84.49 (0.25)	81.93 (0.51)	67.76 (0.41)
	Mixup	89.11 (0.15)	90.83 (0.38)	83.52 (2.61)	73.41 (0.73)	89.52 (0.20)	90.94 (0.32)	80.37 (2.76)	67.97 (0.15)
	GroupDro	89.05 (0.52)	89.49 (2.92)	83.26 (1.57)	74.10 (0.14)	89.22 (0.35)	89.26 (2.79)	79.63 (2.41)	68.07 (0.98)
Refined	ERM	91.99 (0.26)	87.11 (1.50)	85.02 (0.31)	74.41 (0.09)	92.11 (0.20)	86.87 (1.41)	83.17 (0.66)	69.51 (0.30)
	IRM	92.40 (0.12)	89.66 (0.63)	84.12 (0.14)	74.47 (0.15)	92.46 (0.13)	89.49 (0.74)	81.73 (0.21)	69.30 (0.48)
	DeepCoral	92.00 (0.03)	86.24 (0.15)	85.16 (0.33)	74.56 (0.25)	92.16 (0.09)	85.74 (0.24)	83.41 (0.40)	69.27 (0.52)
	DANN	91.61 (0.13)	78.02 (0.54)	85.23 (0.17)	71.29 (0.17)	91.88 (0.15)	77.14 (0.64)	83.42 (0.41)	66.58 (0.29)
	Mixup	92.01 (0.29)	86.58 (1.84)	85.39 (0.08)	74.25 (0.16)	92.18 (0.15)	86.02 (1.95)	83.76 (0.13)	69.29 (0.19)
	GroupDro	92.06 (0.17)	87.14 (0.47)	85.03 (0.16)	74.30 (0.22)	92.26 (0.09)	86.73 (0.33)	83.22 (0.42)	69.40 (0.40)
General	ERM	91.16 (0.18)	85.62 (1.66)	85.61 (0.74)	73.67 (0.08)	90.95 (0.13)	85.34 (1.67)	80.69 (0.95)	68.48 (0.27)
	IRM	90.87 (0.19)	82.78 (2.30)	85.81 (0.11)	73.61 (0.18)	90.70 (0.12)	82.68 (2.40)	80.90 (0.34)	68.43 (0.33)
	DeepCoral	90.82 (0.10)	82.22 (1.96)	86.00 (0.13)	73.34 (0.06)	90.63 (0.07)	81.98 (1.94)	81.04 (0.60)	68.13 (0.73)
	DANN	90.84 (0.03)	80.96 (1.18)	85.90 (0.54)	71.52 (0.24)	90.70 (0.03)	80.20 (1.03)	81.08 (0.82)	66.38 (0.29)
	Mixup	90.98 (0.18)	83.05 (1.63)	86.11 (0.20)	73.49 (0.28)	90.81 (0.19)	82.88 (1.70)	81.32 (0.39)	68.45 (0.14)
	GroupDro	90.77 (0.09)	82.53 (1.30)	85.69 (0.54)	73.36 (0.40)	90.59 (0.10)	82.43 (1.30)	80.49 (1.07)	68.11 (0.38)

mance of OOD is degraded relative to that of ID. On the validation set of core noise level, the OOD performance of ERM degrades by 16.71% in AUC relative to the ID performance, while the performance drop expanded to 21.84% on test set. 2) OOD algorithms designed for computer vision tasks hardly work in SBAP scenarios. The performance of algorithms designed for OOD scenarios are difficult to match the performance of ERM, which means in order to promote the development of AI aided drug discovery, it is necessary to design OOD algorithms with the consideration of characteristics of drug development scenarios. Next, we will further analyze the experimental results from different aspects.

6.2.4 PERFORMANCE GAP OF DIFFERENT DOMAINS

Different domain split methods may result in different distribution shifts, and therefore will also bring different challenges to the algorithms. Here, we analyze 5 built-in domain splits for the SBAP task. Figure 9 shows the performance gap of different domain splits. We conduct analysis under different noise levels and algorithms. The values of gap are calculated on the testing set and averaged over all measurements types. From Figure 9, we can see that: 1) The noise level of the dataset has a great impact on the performance gap of ID and OOD. On one hand, each noise level has a different domain split method that can bring the biggest performance gap across all algorithms. For example, in core noise level, the domain 'protein family' brings the largest performance gap across all algorithms, while it changes to be 'size' in refined noise level. On the other hand, as the noise level increases, the performance gap gradually narrows. Combining with Table 9, we observe that this is caused by the degradation of ID performance. 2) Among all domain split methods, the gap brought by scaffold is relatively small. We speculate that this

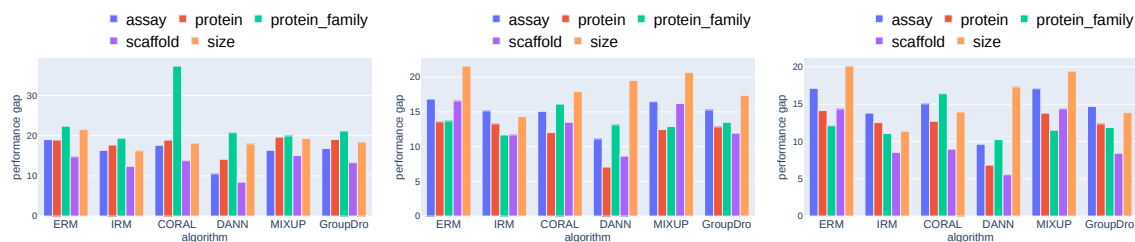


Figure 9: Performance gap on AUC of different domain splits with different noise levels and OOD algorithms on the DrugOOD-sbap datasets. The gap values are calculated on the OOD test set and averaged over four measurement types. Left to right: core noise level, refined noise level, general noise level. Color indicates domain splits for SBAP tasks.

may be due to the fact that scaffold split induces more domain than other split methods, which makes the training set cover a wider portion of the underlying distribution.

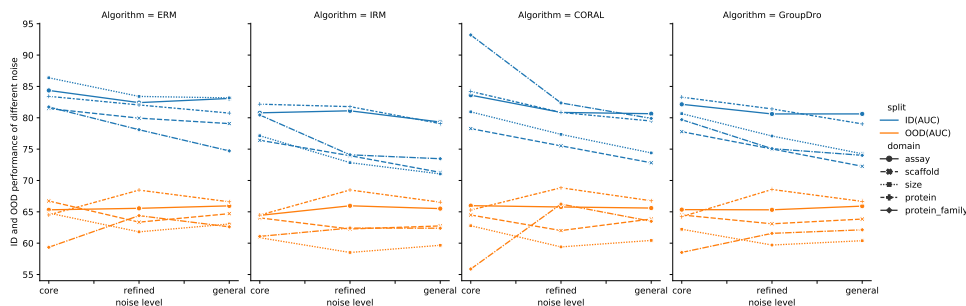


Figure 10: ID and OOD performance with different noise levels. Left to right: ERM, IRM, DeepCoral, GroupDro. Blue color indicates the ID performance while orange color denotes the OOD performance.

6.2.5 STUDY FOR DIFFERENT NOISE LEVELS

Here, we study the effect of different noise levels on ID and OOD performance. Figure 10 shows the ID and OOD performance of 4 algorithms with different noises. The values are averaged over all measurement types. It can be seen that the performance of ID generally decreases with the increase of noise level. The introduction of noise hurts the performance of the model despite the larger amount of data, which suggests that we need to pay more attention to the noise of the data source in the realistic scenario. How to design an algorithm that is robust to both noise and distribution shift is a worthy research direction. As for OOD performance, we can see that different domain split shows different changing trend while the noise level increases. However, we notice that the OOD performance of different algorithms under a particular domain exhibits similar behavior for ERM, which means that existing OOD algorithms do not incorporate the noise of the real scene, nor are they designed to mitigate its impact.

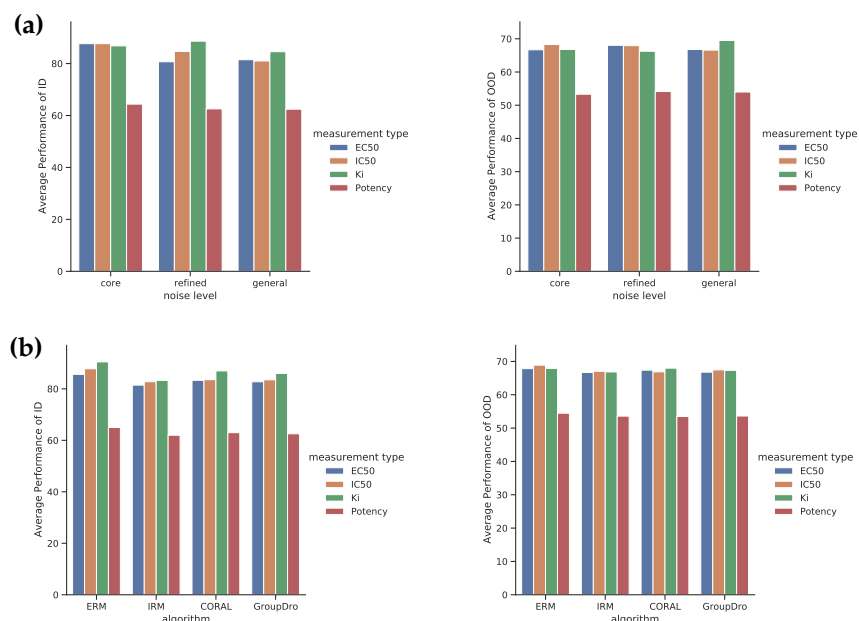


Figure 11: Average performance of ID (left) and OOD (right) for different measurement types. We present the performance of varying measurement types with the change of noise levels (a) and OOD algorithms (b).

6.2.6 STUDY FOR DIFFERENT MEASUREMENT TYPES

The automated dataset curator supports variant measurement types, e.g., EC50, IC50. As different measurement types will generate datasets with different distributions and noise, we analyze the performance of different measurement types by varying the noise levels and algorithms. The results are shown in Figure 11. One can see that: 1) As a result of different measurement types, ID and OOD performance can differ, for example, the Potency measurement is generally low in both ID and OOD, possibly due to the high noise level in the Potency measurement. 2) Our benchmark algorithms are robust to measurement types since they have acceptable accuracy for almost all types of measurement.

7. Discussions and Future Work

In this work we have presented an automated dataset curator and benchmark based on the large-scale bioassay deposition website ChEMBL, in order to facilitate OOD research for AI-aided drug discovery. It is very worthwhile to explore more in the following respects.

As observed in current benchmark results, existing general OOD methods do not significantly outperform the baseline ERM method. Most of these OOD methods are designed and validated with visual and/or textual data, which may fail in capturing critical information for the affinity prediction problem. This implies that to further improve the performance under various out-of-distribution scenarios, it is essential to develop more advanced OOD methods, particularly with drug-related domain knowledge integrated.

Another key characteristic of DrugOOD database is that the majority of data falls into the highest noise level (“general”). Simply discarding such noisy labels and only referring to high-quality ones may severely limit the model performance due to insufficient training data. It could be worth investigating that whether large-scale unsupervised pre-training can be utilized to construct better representations for molecules and target proteins, which are critical to accurate affinity predictions.

Additionally, learning with noisy labels has been extensively studied in the general context, but it may be crucial to take the generation process of noisy affinity annotations into consideration. This includes different experimental precision, measurement types, activity relation annotation types, etc. It is possible that the data quality can be further improved with carefully-designed denoising techniques, so that more accurate affinity prediction models can be trained.

References

- Aliper, Alexander, Plis, Sergey, Artemov, Artem, Ulloa, Alvaro, Mamoshina, Polina, and Zhavoronkov, Alex. Deep learning applications for predicting pharmacological properties of drugs and drug repurposing using transcriptomic data. *Molecular pharmaceuticals*, 13(7):2524–2530, 2016.
- Angluin, Dana and Laird, Philip. Learning from noisy examples. *Machine Learning*, 2(4): 343–370, 1988.
- Arjovsky, Martin, Bottou, Léon, Gulrajani, Ishaan, and Lopez-Paz, David. Invariant risk minimization. *arXiv preprint arXiv:1907.02893*, 2019.
- Asilar, Ece, Hemmerich, Jennifer, and Ecker, Gerhard F. Image based liver toxicity prediction. *Journal of chemical information and modeling*, 60(3):1111–1121, 2020.
- Azadi, Samaneh, Feng, Jiashi, Jegelka, Stefanie, and Darrell, Trevor. Auxiliary image regularization for deep cnns with noisy labels. In *ICLR*, 2016.
- Baek, Minkyung, DiMaio, Frank, Anishchenko, Ivan, Dauparas, Justas, Ovchinnikov, Sergey, Lee, Gyu Rie, Wang, Jue, Cong, Qian, Kinch, Lisa N, Schaeffer, R Dustin, et al. Accurate prediction of protein structures and interactions using a 3-track network. *bioRxiv*, 2021.
- Ballester, Pedro J. and Mitchell, John B. O. A machine learning approach to predicting protein–ligand binding affinity with applications to molecular docking. *Bioinformatics*, 26(9):1169–1175, March 2010. doi: 10.1093/bioinformatics/btq112. URL <https://doi.org/10.1093/bioinformatics/btq112>.
- Bao, Jingxiao, He, Xiao, and Zhang, John ZH. Deepbsp—a machine learning method for accurate prediction of protein–ligand docking structures. *Journal of Chemical Information and Modeling*, 2021.
- Beery, Sara, Van Horn, Grant, and Perona, Pietro. Recognition in terra incognita. In *Proceedings of the European conference on computer vision (ECCV)*, pp. 456–473, 2018.
- Bender, Andreas and Cortés-Ciriano, Isidro. Artificial intelligence in drug discovery: what is realistic, what are illusions? part 1: ways to make an impact, and why we are not there yet. *Drug discovery today*, 26(2):511–524, 2021.
- Brandes, Nadav, Ofer, Dan, Peleg, Yam, Rappoport, Nadav, and Linial, Michal. Proteinbert: A universal deep-learning model of protein sequence and function. *bioRxiv*, 2021.
- Breiman, Leo. Random forests. *Machine learning*, 45(1):5–32, 2001.
- Burden, Frank R. and Winkler, David A. Robust qsar models using bayesian regularized neural networks. *Journal of Medicinal Chemistry*, 42(16):3183–3187, 1999.
- Burley, Stephen K, Bhikadiya, Charmi, Bi, Chunxiao, Bittrich, Sebastian, Chen, Li, Crichlow, Gregg V, Christie, Cole H, Dalenberg, Kenneth, Di Costanzo, Luigi, Duarte,

- Jose M, Dutta, Shuchismita, Feng, Zukang, Ganesan, Sai, Goodsell, David S, Ghosh, Sutapa, Green, Rachel Kramer, Guranović, Vladimir, Guzenko, Dmytro, Hudson, Brian P, Lawson, Catherine L, Liang, Yuhe, Lowe, Robert, Namkoong, Harry, Peisach, Ezra, Persikova, Irina, Randle, Chris, Rose, Alexander, Rose, Yana, Sali, Andrej, Segura, Joan, Sekharan, Monica, Shao, Chenghua, Tao, Yi-Ping, Voigt, Maria, Westbrook, John D, Young, Jasmine Y, Zardecki, Christine, and Zhuravleva, Marina. Rcsb protein data bank: powerful new tools for exploring 3d structures of biological macromolecules for basic and applied research and education in fundamental biology, biomedicine, biotechnology, bioengineering and energy sciences. *Nucleic Acids Research*, 49(D1):D437–D451, 11 2020. ISSN 0305-1048.
- Carlson, Heather A and Dunbar Jr, James B. A call to arms: what you can do for computational drug discovery, 2011.
- Chang, Shiyu, Zhang, Yang, Yu, Mo, and Jaakkola, Tommi. Invariant rationalization. In *International Conference on Machine Learning*, pp. 1448–1458. PMLR, 2020.
- Chen, Binghong, Li, Chengtao, Dai, Hanjun, and Song, Le. Retro*: learning retrosynthetic planning with neural guided a* search. In *International Conference on Machine Learning*, pp. 1608–1616. PMLR, 2020.
- Chen, Kai, Wang, Jiaqi, Pang, Jiangmiao, Cao, Yuhang, Xiong, Yu, Li, Xiaoxiao, Sun, Shuyang, Feng, Wansen, Liu, Ziwei, Xu, Jiarui, Zhang, Zheng, Cheng, Dazhi, Zhu, Chenchen, Cheng, Tianheng, Zhao, Qijie, Li, Buyu, Lu, Xin, Zhu, Rui, Wu, Yue, Dai, Jifeng, Wang, Jingdong, Shi, Jianping, Ouyang, Wanli, Change Loy, Chen, and Lin, Dahua. MMDetection: Open MMLab Detection Toolbox and Benchmark. *arXiv e-prints*, art. arXiv:1906.07155, June 2019.
- Chuang, Ching-Yao and Mroueh, Youssef. Fair mixup: Fairness via interpolation. In *International Conference on Learning Representations*, 2021.
- Coley, Connor W, Rogers, Luke, Green, William H, and Jensen, Klavs F. Computer-assisted retrosynthesis based on molecular similarity. *ACS central science*, 3(12):1237–1245, 2017.
- Consortium, The UniProt. UniProt: a hub for protein information. *Nucleic Acids Research*, 43(D1):D204–D212, 10 2014. ISSN 0305-1048. doi: 10.1093/nar/gku989. URL <https://doi.org/10.1093/nar/gku989>.
- Cortés-Ciriano, Isidro and Bender, Andreas. How consistent are publicly reported cytotoxicity data? large-scale statistical analysis of the concordance of public independent cytotoxicity measurements. *ChemMedChem*, 11(1):57–71, 2016.
- Dahl, George E., Jaitly, Navdeep, and Salakhutdinov, Ruslan. Multi-task neural networks for qsar predictions, 2014.
- Davies, Mark, Nowotka, Michał, Papadatos, George, Dedman, Nathan, Gaulton, Anna, Atkinson, Francis, Bellis, Louisa, and Overington, John P. ChEMBL web services: streamlining access to drug discovery data and utilities. *Nucleic acids research*, 43(W1):W612–W620, Jul 2015. ISSN 1362-4962.

- Deng, Jianyuan, Yang, Zhibo, Ojima, Iwao, Samaras, Dimitris, and Wang, Fusheng. Artificial intelligence in drug discovery: applications and techniques. *arXiv preprint arXiv:2106.05386*, 2021.
- Devlin, Jacob, Chang, Ming-Wei, Lee, Kenton, and Toutanova, Kristina. Bert: Pre-training of deep bidirectional transformers for language understanding. *arXiv preprint arXiv:1810.04805*, 2018.
- Duvenaud, David, Maclaurin, Dougal, Aguilera-Iparraguirre, Jorge, Gómez-Bombarelli, Rafael, Hirzel, Timothy, Aspuru-Guzik, Alán, and Adams, Ryan P. Convolutional networks on graphs for learning molecular fingerprints. In Cortes, Corinna, Lawrence, Neil D., Lee, Daniel D., Sugiyama, Masashi, and Garnett, Roman (eds.), *Advances in Neural Information Processing Systems 28: Annual Conference on Neural Information Processing Systems 2015, December 7-12, 2015, Montreal, Quebec, Canada*, pp. 2224–2232, 2015. URL <https://proceedings.neurips.cc/paper/2015/hash/f9be311e65d81a9ad8150a60844bb94c-Abstract.html>.
- Fang, Chen, Xu, Ye, and Rockmore, Daniel N. Unbiased metric learning: On the utilization of multiple datasets and web images for softening bias. In *Proceedings of the IEEE International Conference on Computer Vision*, pp. 1657–1664, 2013.
- Feinberg, Evan N, Joshi, Elizabeth, Pande, Vijay S, and Cheng, Alan C. Improvement in admet prediction with multitask deep featurization. *Journal of medicinal chemistry*, 63(16):8835–8848, 2020.
- Ganin, Yaroslav, Ustinova, Evgeniya, Ajakan, Hana, Germain, Pascal, Larochelle, Hugo, Laviolette, Francois, Marchand, Mario, and Lempitsky, Victor. Domain-adversarial training of neural networks. *The journal of machine learning research*, 17(1):2096–2030, 2016.
- Gao, Wenhao, Mahajan, Sai Pooja, Sulam, Jeremias, and Gray, Jeffrey J. Deep learning in protein structural modeling and design. *Patterns*, pp. 100142, 2020.
- Ghifary, Muhammad, Kleijn, W Bastiaan, Zhang, Mengjie, and Balduzzi, David. Domain generalization for object recognition with multi-task autoencoders. In *Proceedings of the IEEE International Conference on Computer Vision*, pp. 2551–2559, 2015.
- Gilmer, Justin, Schoenholz, Samuel S, Riley, Patrick F, Vinyals, Oriol, and Dahl, George E. Neural message passing for quantum chemistry. In *International Conference on Machine Learning*, pp. 1263–1272. PMLR, 2017.
- Gilson, Michael K, Liu, Tiqing, Baitaluk, Michael, Nicola, George, Hwang, Linda, and Chong, Jenny. Bindingdb in 2015: a public database for medicinal chemistry, computational chemistry and systems pharmacology. *Nucleic acids research*, 44(D1):D1045–D1053, 2016.
- Glen, Robert C, Bender, Andreas, Arnby, Catrin H, Carlsson, Lars, Boyer, Scott, and Smith, James. Circular fingerprints: flexible molecular descriptors with applications from physical chemistry to adme. *IDrugs*, 9(3):199, 2006.

- Goel, Karan, Gu, Albert, Li, Yixuan, and Ré, Christopher. Model patching: Closing the subgroup performance gap with data augmentation. *arXiv preprint arXiv:2008.06775*, 2020.
- Goh, Garrett B, Hodas, Nathan O, Siegel, Charles, and Vishnu, Abhinav. Smiles2vec: An interpretable general-purpose deep neural network for predicting chemical properties. *arXiv preprint arXiv:1712.02034*, 2017.
- Gulrajani, Ishaan and Lopez-Paz, David. In search of lost domain generalization. *arXiv preprint arXiv:2007.01434*, 2020.
- Gysi, Deisy Morselli, Do Valle, Ítalo, Zitnik, Marinka, Ameli, Asher, Gan, Xiao, Varol, Onur, Ghiassian, Susan Dina, Patten, JJ, Davey, Robert A, Loscalzo, Joseph, et al. Network medicine framework for identifying drug-repurposing opportunities for covid-19. *Proceedings of the National Academy of Sciences*, 118(19), 2021.
- Han, Bo, Yao, Jiangchao, Niu, Gang, Zhou, Mingyuan, Tsang, Ivor, Zhang, Ya, and Sugiyama, Masashi. Masking: A new perspective of noisy supervision. In *NeurIPS*, pp. 5836–5846, 2018a.
- Han, Bo, Yao, Quanming, Yu, Xingrui, Niu, Gang, Xu, Miao, Hu, Weihua, Tsang, Ivor, and Sugiyama, Masashi. Co-teaching: Robust training of deep neural networks with extremely noisy labels. In *NeurIPS*, pp. 8527–8537, 2018b.
- Han, Bo, Yao, Quanming, Liu, Tongliang, Niu, Gang, Tsang, Ivor W, Kwok, James T, and Sugiyama, Masashi. A survey of label-noise representation learning: Past, present and future. *arXiv preprint arXiv:2011.04406*, 2020.
- Han, Jiangfan, Luo, Ping, and Wang, Xiaogang. Deep self-learning from noisy labels. In *ICCV*, 2019.
- He, Yue, Shen, Zheyang, and Cui, Peng. Towards non-iid image classification: A dataset and baselines. *Pattern Recognition*, 110:107383, 2021.
- Hirohara, Maya, Saito, Yutaka, Koda, Yuki, Sato, Kengo, and Sakakibara, Yasubumi. Convolutional neural network based on smiles representation of compounds for detecting chemical motif. *BMC bioinformatics*, 19(19):83–94, 2018.
- Hu, Peng-Wei, Chan, Keith CC, and You, Zhu-Hong. Large-scale prediction of drug-target interactions from deep representations. In *2016 international joint conference on neural networks (IJCNN)*, pp. 1236–1243. IEEE, 2016.
- Hu, Ruifeng, Xu, Haodong, Jia, Peilin, and Zhao, Zhongming. KinaseMD: kinase mutations and drug response database. *Nucleic Acids Research*, 49(D1):D552–D561, 11 2020. ISSN 0305-1048. doi: 10.1093/nar/gkaa945. URL <https://doi.org/10.1093/nar/gkaa945>.
- Hu, Weihua, Fey, Matthias, Zitnik, Marinka, Dong, Yuxiao, Ren, Hongyu, Liu, Bowen, Catasta, Michele, and Leskovec, Jure. Open Graph Benchmark: Datasets for Machine Learning on Graphs. *arXiv e-prints*, art. arXiv:2005.00687, May 2020.

- Huang, Kexin, Fu, Tianfan, Gao, Wenhao, Zhao, Yue, Roohani, Yusuf, Leskovec, Jure, Coley, Connor W, Xiao, Cao, Sun, Jimeng, and Zitnik, Marinka. Therapeutics data commons: machine learning datasets and tasks for therapeutics. *arXiv preprint arXiv:2102.09548*, 2021.
- Issa, Naiem T, Stathias, Vasileios, Schürer, Stephan, and Dakshanamurthy, Sivanesan. Machine and deep learning approaches for cancer drug repurposing. In *Seminars in cancer biology*, volume 68, pp. 132–142. Elsevier, 2021.
- Jiang, Dejun, Hsieh, Chang-Yu, Wu, Zhenxing, Kang, Yu, Wang, Jike, Wang, Ercheng, Liao, Ben, Shen, Chao, Xu, Lei, Wu, Jian, Cao, Dongsheng, and Hou, Tingjun. InteractionGraphNet: A novel and efficient deep graph representation learning framework for accurate protein–ligand interaction predictions. *Journal of Medicinal Chemistry*, 64(24):18209–18232, December 2021. doi: 10.1021/acs.jmedchem.1c01830. URL <https://doi.org/10.1021/acs.jmedchem.1c01830>.
- Jiang, Lu, Zhou, Zhengyuan, Leung, Thomas, Li, Li-Jia, and Fei-Fei, Li. Mentornet: Learning data-driven curriculum for very deep neural networks on corrupted labels. In *ICML*, pp. 2304–2313, 2018.
- Jiménez, José, Skalic, Miha, Martinez-Rosell, Gerard, and De Fabritiis, Gianni. K deep: protein–ligand absolute binding affinity prediction via 3d-convolutional neural networks. *Journal of chemical information and modeling*, 58(2):287–296, 2018.
- Jing, Yankang, Bian, Yuemin, Hu, Ziheng, Wang, Lirong, and Xie, Xiang-Qun Sean. Deep learning for drug design: an artificial intelligence paradigm for drug discovery in the big data era. *The AAPS journal*, 20(3):1–10, 2018.
- Johnson, M. A. and Maggiora, G. M. Concepts and applications of molecular similarity. *Wiley*, 1990.
- Jumper, John, Evans, Richard, Pritzel, Alexander, Green, Tim, Figurnov, Michael, Ronneberger, Olaf, Tunyasuvunakool, Kathryn, Bates, Russ, Zidek, Augustin, Potapenko, Anna, et al. Highly accurate protein structure prediction with alphafold. *Nature*, 596(7873):583–589, 2021.
- Karimi, Mostafa, Wu, Di, Wang, Zhangyang, and Shen, Yang. Deepaffinity: interpretable deep learning of compound–protein affinity through unified recurrent and convolutional neural networks. *Bioinformatics*, 35(18):3329–3338, 2019.
- Kearnes, Steven, McCloskey, Kevin, Berndl, Marc, Pande, Vijay, and Riley, Patrick. Molecular graph convolutions: moving beyond fingerprints. *Journal of computer-aided molecular design*, 30(8):595–608, 2016.
- Keiser, Michael J., Roth, Bryan L., Armbruster, Blaine N., Ernsberger, Paul, Irwin, John J., and Shoichet, Brian K. Relating protein pharmacology by ligand chemistry. *Nature Biotechnology*, 25(2):197–206, Feb 2007. ISSN 1546-1696. doi: 10.1038/nbt1284. URL <https://doi.org/10.1038/nbt1284>.

- Kim, Ryangguk and Skolnick, Jeffrey. Assessment of programs for ligand binding affinity prediction. *Journal of Computational Chemistry*, 29(8):1316–1331, 2008.
- Kipf, Thomas N and Welling, Max. Semi-supervised classification with graph convolutional networks. *arXiv preprint arXiv:1609.02907*, 2016.
- Kleinbaum, David G, Dietz, K, Gail, M, Klein, Mitchel, and Klein, Mitchell. *Logistic regression*. Springer, 2002.
- Koes, David Ryan, Baumgartner, Matthew P, and Camacho, Carlos J. Lessons learned in empirical scoring with smina from the csar 2011 benchmarking exercise. *Journal of chemical information and modeling*, 53(8):1893–1904, 2013.
- Koh, Pang Wei, Sagawa, Shiori, Marklund, Henrik, Xie, Sang Michael, Zhang, Marvin, Balsubramani, Akshay, Hu, Weihua, Yasunaga, Michihiro, Phillips, Richard Lanas, Gao, Irena, Lee, Tony, David, Etienne, Stavness, Ian, Guo, Wei, Earnshaw, Berton, Haque, Imran, Beery, Sara M, Leskovec, Jure, Kundaje, Anshul, Pierson, Emma, Levine, Sergey, Finn, Chelsea, and Liang, Percy. Wilds: A benchmark of in-the-wild distribution shifts. In Meila, Marina and Zhang, Tong (eds.), *Proceedings of the 38th International Conference on Machine Learning*, volume 139 of *Proceedings of Machine Learning Research*, pp. 5637–5664. PMLR, 18–24 Jul 2021. URL <https://proceedings.mlr.press/v139/koh21a.html>.
- Koyama, Masanori and Yamaguchi, Shoichiro. Out-of-distribution generalization with maximal invariant predictor. *arXiv preprint arXiv:2008.01883*, 2020.
- Koyama, Masanori and Yamaguchi, Shoichiro. When is invariance useful in an out-of-distribution generalization problem ?, 2021.
- Kramer, Christian, Kalliokoski, Tuomo, Geddeck, Peter, and Vulpetti, Anna. The experimental uncertainty of heterogeneous public k i data. *Journal of medicinal chemistry*, 55(11):5165–5173, 2012.
- Krueger, David, Caballero, Ethan, Jacobsen, Joern-Henrik, Zhang, Amy, Binas, Jonathan, Zhang, Dinghuai, Le Priol, Remi, and Courville, Aaron. Out-of-distribution generalization via risk extrapolation (rex). In *International Conference on Machine Learning*, pp. 5815–5826. PMLR, 2021a.
- Krueger, David, Caballero, Ethan, Jacobsen, Joern-Henrik, Zhang, Amy, Binas, Jonathan, Zhang, Dinghuai, Priol, Remi Le, and Courville, Aaron. Out-of-distribution generalization via risk extrapolation (rex). In *Proceedings of the 38th International Conference on Machine Learning*, volume 139, pp. 5815–5826. PMLR, Jul 2021b.
- Kwon, Sunyoung, Bae, Ho, Jo, Jeonghee, and Yoon, Sungroh. Comprehensive ensemble in qsar prediction for drug discovery. *BMC Bioinformatics*, 20(1):521, Oct 2019. ISSN 1471-2105. doi: 10.1186/s12859-019-3135-4. URL <https://doi.org/10.1186/s12859-019-3135-4>.
- Laine, Samuli and Aila, Timo. Temporal ensembling for semi-supervised learning. In *ICLR*, 2017.

- Landrum, Greg. Rdkit: A software suite for cheminformatics, computational chemistry, and predictive modeling, 2013.
- Lazic, Stanley E and Williams, Dominic P. Quantifying sources of uncertainty in drug discovery predictions with probabilistic models. *Artificial Intelligence in the Life Sciences*, pp. 100004, 2021.
- Li, Da, Yang, Yongxin, Song, Yi-Zhe, and Hospedales, Timothy M. Deeper, broader and artier domain generalization. In *Proceedings of the IEEE international conference on computer vision*, pp. 5542–5550, 2017.
- Li, Haoliang, Pan, Sinno Jialin, Wang, Shiqi, and Kot, Alex C. Domain generalization with adversarial feature learning. In *Proceedings of the IEEE Conference on Computer Vision and Pattern Recognition*, pp. 5400–5409, 2018.
- Li, Junnan, Socher, Richard, and Hoi, Steven CH. Dividemix: Learning with noisy labels as semi-supervised learning. In *ICLR*, 2020.
- Li, Mufei, Zhou, Jinjing, Hu, Jiajing, Fan, Wenxuan, Zhang, Yangkang, Gu, Yaxin, and Karypis, George. Dgl-lifesci: An open-source toolkit for deep learning on graphs in life science. *ACS omega*, 6(41):27233–27238, 2021a.
- Li, Shuangli, Zhou, Jingbo, Xu, Tong, Huang, Liang, Wang, Fan, Xiong, Haoyi, Huang, Weili, Dou, Dejing, and Xiong, Hui. Structure-aware interactive graph neural networks for the prediction of protein-ligand binding affinity. In *Proceedings of the 27th ACM SIGKDD Conference on Knowledge Discovery & Data Mining*, pp. 975–985, 2021b.
- Lim, Jaechang, Ryu, Seongok, Park, Kyubyong, Choe, Yo Joong, Ham, Jiyeon, and Kim, Woo Youn. Predicting drug–target interaction using a novel graph neural network with 3d structure-embedded graph representation. *Journal of chemical information and modeling*, 59(9):3981–3988, 2019.
- Lim, Sangsoo, Lu, Yijingxiu, Cho, Chang Yun, Sung, Inyoung, Kim, Jungwoo, Kim, Youngkuk, Park, Sungjoon, and Kim, Sun. A review on compound-protein interaction prediction methods: Data, format, representation and model. *Computational and Structural Biotechnology Journal*, 19:1541, 2021.
- Liu, Tongliang and Tao, Dacheng. Classification with noisy labels by importance reweighting. *TPAMI*, 38(3):447–461, 2015.
- Liu, Zhihai, Li, Yan, Han, Li, Li, Jie, Liu, Jie, Zhao, Zhixiong, Nie, Wei, Liu, Yuchen, and Wang, Renxiao. Pdb-wide collection of binding data: current status of the pddbnd database. *Bioinformatics*, 31(3):405–412, 10 2014. ISSN 1367-4803.
- Liu, Ziwei, Luo, Ping, Wang, Xiaogang, and Tang, Xiaoou. Deep learning face attributes in the wild. In *Proceedings of the IEEE international conference on computer vision*, pp. 3730–3738, 2015.

- Long, Mingsheng, Cao, Yue, Wang, Jianmin, and Jordan, Michael. Learning transferable features with deep adaptation networks. In *International conference on machine learning*, pp. 97–105. PMLR, 2015.
- Lu, Chengqiang, Liu, Qi, Wang, Chao, Huang, Zhenya, Lin, Peize, and He, Lixin. Molecular property prediction: A multilevel quantum interactions modeling perspective. In *Proceedings of the AAAI Conference on Artificial Intelligence*, volume 33, pp. 1052–1060, 2019.
- Luco, Juan M. and Ferretti, Ferdinando H. Qsar based on multiple linear regression and pls methods for the anti-hiv activity of a large group of hept derivatives. *Journal of Chemical Information and Computer Sciences*, 37(2):392–401, 1997.
- Lukasik, Michal, Bhojanapalli, Srinadh, Menon, Aditya Krishna, and Kumar, Sanjiv. Does label smoothing mitigate label noise? In *ICML*, 2020.
- Ma, Hehuan, Bian, Yatao, Rong, Yu, Huang, Wenbing, Xu, Tingyang, Xie, Weiyang, Ye, Geyan, and Huang, Junzhou. Multi-view graph neural networks for molecular property prediction. *arXiv preprint arXiv:2005.13607*, 2020.
- Mamoshina, Polina, Volosnikova, Marina, Ozerov, Ivan V, Putin, Evgeny, Skibina, Ekaterina, Cortese, Franco, and Zhavoronkov, Alex. Machine learning on human muscle transcriptomic data for biomarker discovery and tissue-specific drug target identification. *Frontiers in genetics*, 9:242, 2018.
- Martin, Eric J., Polyakov, Valery R., Tian, Li, and Perez, Rolando C. Profile-qsar 2.0: Kinase virtual screening accuracy comparable to four-concentration ic50s for realistically novel compounds. *Journal of Chemical Information and Modeling*, 57(8):2077–2088, 2017. doi: 10.1021/acs.jcim.7b00166. URL <https://doi.org/10.1021/acs.jcim.7b00166>. PMID: 28651433.
- Mayr, Andreas, Klambauer, Günter, Unterthiner, Thomas, Steijaert, Marvin, Wegner, Jörg K, Ceulemans, Hugo, Clevert, Djork-Arné, and Hochreiter, Sepp. Large-scale comparison of machine learning methods for drug target prediction on chembl. *Chemical science*, 9(24):5441–5451, 2018.
- McNutt, Andrew T, Francoeur, Paul, Aggarwal, Rishal, Masuda, Tomohide, Meli, Rocco, Ragoza, Matthew, Sunseri, Jocelyn, and Koes, David Ryan. Glna 1.0: molecular docking with deep learning. *Journal of cheminformatics*, 13(1):1–20, 2021.
- Mendez, David, Gaulton, Anna, Bento, A Patrícia, Chambers, Jon, De Veij, Marleen, Félix, Eloy, Magariños, María Paula, Mosquera, Juan F, Mutowo, Prudence, Nowotka, Michał, et al. ChEMBL: towards direct deposition of bioassay data. *Nucleic acids research*, 47(D1): D930–D940, 2019.
- Min, Seonwoo, Park, Seunghyun, Kim, Siwon, Choi, Hyun-Soo, Lee, Byunghan, and Yoon, Sungroh. Pre-training of deep bidirectional protein sequence representations with structural information. *IEEE Access*, 9:123912–123926, 2021.

- Morgan, HL. The generation of a unique machine description for chemical structures—a technique developed at chemical abstracts service. *J. Chemical Documentation*, 5:107–113, 1965.
- Muratov, Eugene N, Bajorath, Jürgen, Sheridan, Robert P, Tetko, Igor V, Filimonov, Dmitry, Poroikov, Vladimir, Oprea, Tudor I, Baskin, Igor I, Varnek, Alexandre, Roitberg, Adrian, et al. Qsar without borders. *Chemical Society Reviews*, 49(11):3525–3564, 2020.
- Nosengo, Nicola. Can you teach old drugs new tricks? *Nature News*, 534(7607):314, 2016.
- Pan, Sinno Jialin and Yang, Qiang. A survey on transfer learning. *IEEE Transactions on knowledge and data engineering*, 22(10):1345–1359, 2009.
- Paul, Debleena, Sanap, Gaurav, Shenoy, Snehal, Kalyane, Dnyaneshwar, Kalia, Kiran, and Tekade, Rakesh K. Artificial intelligence in drug discovery and development. *Drug Discovery Today*, 26(1):80, 2021.
- Peng, Xingchao, Bai, Qinxun, Xia, Xide, Huang, Zijun, Saenko, Kate, and Wang, Bo. Moment matching for multi-source domain adaptation. In *Proceedings of the IEEE/CVF International Conference on Computer Vision*, pp. 1406–1415, 2019.
- Pham, Thai-Hoang, Qiu, Yue, Zeng, Jucheng, Xie, Lei, and Zhang, Ping. A deep learning framework for high-throughput mechanism-driven phenotype compound screening and its application to covid-19 drug repurposing. *Nature Machine Intelligence*, 3(3): 247–257, 2021.
- Pradeep, Prachi, Povinelli, Richard J, White, Shannon, and Merrill, Stephen J. An ensemble model of qsar tools for regulatory risk assessment. *Journal of Cheminformatics*, 8(1): 1–9, 2016.
- Pushpakom, Sudeep, Iorio, Francesco, Eyers, Patrick A, Escott, K Jane, Hopper, Shirley, Wells, Andrew, Doig, Andrew, Williams, Tim, Latimer, Joanna, McNamee, Christine, et al. Drug repurposing: progress, challenges and recommendations. *Nature reviews Drug discovery*, 18(1):41–58, 2019.
- Qiao, Fengchun, Zhao, Long, and Peng, Xi. Learning to learn single domain generalization. In *Proceedings of the IEEE/CVF Conference on Computer Vision and Pattern Recognition (CVPR)*, June 2020.
- Ramsundar, Bharath, Kearnes, Steven, Riley, Patrick, Webster, Dale, Konerding, David, and Pande, Vijay. Massively multitask networks for drug discovery. *arXiv preprint arXiv:1502.02072*, 2015.
- Ren, Mengye, Zeng, Wenyuan, Yang, Bin, and Urtasun, Raquel. Learning to reweight examples for robust deep learning. In *ICML*, 2018.
- Rogers, David and Hahn, Mathew. Extended-connectivity fingerprints. *Journal of chemical information and modeling*, 50(5):742–754, 2010.

- Romera-Paredes, Bernardino and Torr, Philip. An embarrassingly simple approach to zero-shot learning. In *International conference on machine learning*, pp. 2152–2161. PMLR, 2015.
- Rong, Yu, Bian, Yatao, Xu, Tingyang, Xie, Weiyang, Wei, Ying, Huang, Wenbing, and Huang, Junzhou. Self-supervised graph transformer on large-scale molecular data. In *NeurIPS*, 2020.
- Roth, Bryan L, Lopez, Estelle, Patel, Shamil, and Kroeze, Wesley K. The multiplicity of serotonin receptors: uselessly diverse molecules or an embarrassment of riches? *The Neuroscientist*, 6(4):252–262, 2000.
- Sagawa, Shiori, Koh, Pang Wei, Hashimoto, Tatsunori B, and Liang, Percy. Distributionally robust neural networks for group shifts: On the importance of regularization for worst-case generalization. *arXiv preprint arXiv:1911.08731*, 2019.
- Sagawa, Shiori, Raghunathan, Aditi, Koh, Pang Wei, and Liang, Percy. An investigation of why overparameterization exacerbates spurious correlations. In *International Conference on Machine Learning*, pp. 8346–8356. PMLR, 2020.
- Sagawa, Shiori, Koh, Pang Wei, Lee, Tony, Gao, Irena, Xie, Sang Michael, Shen, Kendrick, Kumar, Ananya, Hu, Weihua, Yasunaga, Michihiro, Marklund, Henrik, et al. Extending the wilds benchmark for unsupervised adaptation. *arXiv preprint arXiv:2112.05090*, 2021.
- Sanchez-Lengeling, Benjamin, Outeiral, Carlos, Guimaraes, Gabriel L, and Aspuru-Guzik, Alán. Optimizing distributions over molecular space. an objective-reinforced generative adversarial network for inverse-design chemistry (organic). 2017.
- Sanger, Frederick. The arrangement of amino acids in proteins. *Advances in protein chemistry*, 7:1–67, 1952.
- Satorras, Victor Garcia, Hoogeboom, Emiel, Fuchs, Fabian B, Posner, Ingmar, and Welling, Max. E(n) equivariant normalizing flows for molecule generation in 3d. *arXiv preprint arXiv:2105.09016*, 2021.
- Schneider, Gisbert. Automating drug discovery. *Nature reviews drug discovery*, 17(2):97–113, 2018.
- Schütt, Kristof T, Kindermans, Pieter-Jan, Sauceda, Huziel E, Chmiela, Stefan, Tkatchenko, Alexandre, and Müller, Klaus-Robert. Schnet: A continuous-filter convolutional neural network for modeling quantum interactions. *arXiv preprint arXiv:1706.08566*, 2017.
- Segler, Marwin HS, Preuss, Mike, and Waller, Mark P. Planning chemical syntheses with deep neural networks and symbolic ai. *Nature*, 555(7698):604–610, 2018.
- Shu, Yang, Cao, Zhangjie, Wang, Chenyu, Wang, Jianmin, and Long, Mingsheng. Open domain generalization with domain-augmented meta-learning. In *Proceedings of the IEEE/CVF Conference on Computer Vision and Pattern Recognition*, pp. 9624–9633, 2021.

- Simonovsky, Martin and Komodakis, Nikos. GraphVAE: Towards generation of small graphs using variational autoencoders. In *International conference on artificial neural networks*, pp. 412–422. Springer, 2018.
- Sliwoski, Gregory, Kothiwale, Sandeepkumar, Meiler, Jens, and Lowe Jr., Edward W. Computational methods in drug discovery. *Pharmacological reviews*, 66(1):334–395, Dec 2013. ISSN 1521-0081. doi: 10.1124/pr.112.007336. URL <https://pubmed.ncbi.nlm.nih.gov/24381236>. 24381236[pmid].
- Song, Hwanjun, Kim, Minseok, Park, Dongmin, and Lee, Jae-Gil. Learning from noisy labels with deep neural networks: A survey. *arXiv preprint arXiv:2007.08199*, 2020a.
- Song, Ying, Zheng, Shuangjia, Niu, Zhangming, Fu, Zhang-Hua, Lu, Yutong, and Yang, Yuedong. Communicative representation learning on attributed molecular graphs. In *IJCAI*, pp. 2831–2838, 2020b.
- Stanley, Megan, Bronskill, John F, Maziarz, Krzysztof, Misztela, Hubert, Lanini, Jessica, Segler, Marwin, Schneider, Nadine, and Brockschmidt, Marc. FS-mol: A few-shot learning dataset of molecules. In *Thirty-fifth Conference on Neural Information Processing Systems Datasets and Benchmarks Track (Round 2)*, 2021. URL <https://openreview.net/forum?id=701FtuyLlAd>.
- Stepniewska-Dziubinska, Marta M, Zielenkiewicz, Piotr, and Siedlecki, Pawel. Development and evaluation of a deep learning model for protein–ligand binding affinity prediction. *Bioinformatics*, 34(21):3666–3674, 2018.
- Stokes, Jonathan M, Yang, Kevin, Swanson, Kyle, Jin, Wengong, Cubillos-Ruiz, Andres, Donghia, Nina M, MacNair, Craig R, French, Shawn, Carfrae, Lindsey A, Bloom-Ackermann, Zohar, et al. A deep learning approach to antibiotic discovery. *Cell*, 180(4): 688–702, 2020.
- Sukhbaatar, Sainbayar, Bruna, Joan, Paluri, Manohar, Bourdev, Lubomir, and Fergus, Rob. Training convolutional networks with noisy labels. In *ICLR Workshop*, 2015.
- Sun, Baochen and Saenko, Kate. Deep coral: Correlation alignment for deep domain adaptation. In *European conference on computer vision*, pp. 443–450. Springer, 2016.
- Svetnik, Vladimir, Liaw, Andy, Tong, Christopher, Culberson, J. Christopher, Sheridan, Robert P., and Feuston, Bradley P. Random forest: A classification and regression tool for compound classification and qsar modeling. *Journal of Chemical Information and Computer Sciences*, 43(6):1947–1958, 2003.
- Swamidass, S Joshua, Azencott, Chloé-Agathe, Lin, Ting-Wan, Gramajo, Hugo, Tsai, Shiou-Chuan, and Baldi, Pierre. Influence relevance voting: an accurate and interpretable virtual high throughput screening method. *Journal of chemical information and modeling*, 49(4):756–766, 2009.
- Trott, Oleg and Olson, Arthur J. Autodock vina: improving the speed and accuracy of docking with a new scoring function, efficient optimization, and multithreading. *Journal of computational chemistry*, 31(2):455–461, 2010.

- Tzeng, Eric, Hoffman, Judy, Zhang, Ning, Saenko, Kate, and Darrell, Trevor. Deep domain confusion: Maximizing for domain invariance, 2014.
- van Rooyen, Brendan and Williamson, Robert C. A theory of learning with corrupted labels. *JMLR*, 18(1):8501–8550, 2017.
- van Rooyen, Brendan, Menon, Aditya, and Williamson, Robert. Learning with symmetric label noise: The importance of being unhinged. In *NeurIPS*, pp. 10–18, 2015.
- Vapnik, Vladimir. *The nature of statistical learning theory*. Springer science & business media, 1999.
- Velickovic, Petar, Cucurull, Guillem, Casanova, Arantxa, Romero, Adriana, Liò, Pietro, and Bengio, Yoshua. Graph attention networks. 2018. URL <https://openreview.net/forum?id=rJXMpikCZ>.
- Venkateswara, Hemanth, Eusebio, Jose, Chakraborty, Shayok, and Panchanathan, Sethuraman. Deep hashing network for unsupervised domain adaptation. In *Proceedings of the IEEE conference on computer vision and pattern recognition*, pp. 5018–5027, 2017.
- Volpi, Riccardo, Namkoong, Hongseok, Sener, Ozan, Duchi, John, Murino, Vittorio, and Savarese, Silvio. Generalizing to unseen domains via adversarial data augmentation. *arXiv preprint arXiv:1805.12018*, 2018.
- Wallach, Izhar, Dzamba, Michael, and Heifets, Abraham. Atomnet: a deep convolutional neural network for bioactivity prediction in structure-based drug discovery. *arXiv preprint arXiv:1510.02855*, 2015.
- Wang, Hongwei, Li, Weijiang, Jin, Xiaomeng, Cho, Kyunghyun, Ji, Heng, Han, Jiawei, and Burke, Martin D. Chemical-reaction-aware molecule representation learning. *arXiv preprint arXiv:2109.09888*, 2021.
- Wang, Sheng, Guo, Yuzhi, Wang, Yuhong, Sun, Hongmao, and Huang, Junzhou. Smilesbert: large scale unsupervised pre-training for molecular property prediction. In *Proceedings of the 10th ACM international conference on bioinformatics, computational biology and health informatics*, pp. 429–436, 2019a.
- Wang, Wei, Zheng, Vincent W, Yu, Han, and Miao, Chunyan. A survey of zero-shot learning: Settings, methods, and applications. *ACM Transactions on Intelligent Systems and Technology (TIST)*, 10(2):1–37, 2019b.
- Wang, Yanli, Xiao, Jewen, Suzek, Tugba O, Zhang, Jian, Wang, Jiyao, and Bryant, Stephen H. Pubchem: a public information system for analyzing bioactivities of small molecules. *Nucleic acids research*, 37(suppl_2):W623–W633, 2009.
- Wang, Yixin, Kucukelbir, Alp, and Blei, David M. Robust probabilistic modeling with bayesian data reweighting. In *ICML*, pp. 3646–3655, 2017.
- Wang, Yufei, Li, Haoliang, and Kot, Alex C. Heterogeneous domain generalization via domain mixup. In *ICASSP 2020-2020 IEEE International Conference on Acoustics, Speech and Signal Processing (ICASSP)*, pp. 3622–3626. IEEE, 2020.

- Weininger, David. Smiles, a chemical language and information system. 1. introduction to methodology and encoding rules. *Journal of chemical information and computer sciences*, 28(1):31–36, 1988.
- Wu, Zhenqin, Ramsundar, Bharath, Feinberg, Evan N, Gomes, Joseph, Geniesse, Caleb, Pappu, Aneesh S, Leswing, Karl, and Pande, Vijay. Moleculenet: a benchmark for molecular machine learning. *Chemical science*, 9(2):513–530, 2018.
- Xiong, Zhaoping, Wang, Dingyan, Liu, Xiaohong, Zhong, Feisheng, Wan, Xiaozhe, Li, Xutong, Li, Zhaojun, Luo, Xiaomin, Chen, Kaixian, Jiang, Hualiang, et al. Pushing the boundaries of molecular representation for drug discovery with the graph attention mechanism. *Journal of medicinal chemistry*, 63(16):8749–8760, 2019.
- Xu, Keyulu, Hu, Weihua, Leskovec, Jure, and Jegelka, Stefanie. How powerful are graph neural networks? In *International Conference on Learning Representations*, 2018.
- Xu, Minghao, Zhang, Jian, Ni, Bingbing, Li, Teng, Wang, Chengjie, Tian, Qi, and Zhang, Wenjun. Adversarial domain adaptation with domain mixup. In *The Thirty-Fourth AAAI Conference on Artificial Intelligence*, pp. 6502–6509. AAAI Press, 2020.
- Xu, Zheng, Wang, Sheng, Zhu, Feiyun, and Huang, Junzhou. Seq2seq fingerprint: An unsupervised deep molecular embedding for drug discovery. In *BCB*, 2017.
- Yan, Chaochao, Ding, Qianggang, Zhao, Peilin, Zheng, Shuangjia, Yang, Jinyu, Yu, Yang, and Huang, Junzhou. Retroxpert: Decompose retrosynthesis prediction like a chemist. *arXiv preprint arXiv:2011.02893*, 2020a.
- Yan, Shen, Song, Huan, Li, Nanxiang, Zou, Lincan, and Ren, Liu. Improve unsupervised domain adaptation with mixup training, 2020b.
- Yang, Kevin, Swanson, Kyle, Jin, Wengong, Coley, Connor, Eiden, Philipp, Gao, Hua, Guzman-Perez, Angel, Hopper, Timothy, Kelley, Brian, Mathea, Miriam, et al. Analyzing learned molecular representations for property prediction. *Journal of chemical information and modeling*, 59(8):3370–3388, 2019a.
- Yang, Xin, Wang, Yifei, Byrne, Ryan, Schneider, Gisbert, and Yang, Shengyong. Concepts of artificial intelligence for computer-assisted drug discovery. *Chemical reviews*, 119(18): 10520–10594, 2019b.
- Yao, Huaxiu, Wang, Yu, Li, Sai, Zhang, Linjun, Liang, Weixin, Zou, James, and Finn, Chelsea. Improving out-of-distribution robustness via selective augmentation, 2022.
- Ye, Nanyang, Li, Kaican, Hong, Lanqing, Bai, Haoyue, Chen, Yiting, Zhou, Fengwei, and Li, Zhenguo. Ood-bench: Benchmarking and understanding out-of-distribution generalization datasets and algorithms. *arXiv preprint arXiv:2106.03721*, 2021.
- Ying, Chengxuan, Cai, Tianle, Luo, Shengjie, Zheng, Shuxin, Ke, Guolin, He, Di, Shen, Yanming, and Liu, Tie-Yan. Do transformers really perform bad for graph representation? *arXiv preprint arXiv:2106.05234*, 2021.

- Yu, Xingrui, Han, Bo, Yao, Jiangchao, Niu, Gang, Tsang, Ivor W, and Sugiyama, Masashi. How does disagreement help generalization against label corruption? In *ICML*, 2019.
- Yue, Xiangyu, Zhang, Yang, Zhao, Sicheng, Sangiovanni-Vincentelli, Alberto, Keutzer, Kurt, and Gong, Boqing. Domain randomization and pyramid consistency: Simulation-to-real generalization without accessing target domain data. In *Proceedings of the IEEE/CVF International Conference on Computer Vision*, pp. 2100–2110, 2019.
- Zakharov, Alexey V, Varlamova, Ekaterina V, Lagunin, Alexey A, Dmitriev, Alexander V, Muratov, Eugene N, Fourches, Denis, Kuz'min, Victor E, Poroikov, Vladimir V, Tropsha, Alexander, and Nicklaus, Marc C. Qsar modeling and prediction of drug-drug interactions. *Molecular pharmaceutics*, 13(2):545–556, 2016.
- Zeng, Xiangxiang, Zhu, Siyi, Lu, Weiqiang, Liu, Zehui, Huang, Jin, Zhou, Yadi, Fang, Jiansong, Huang, Yin, Guo, Huimin, Li, Lang, et al. Target identification among known drugs by deep learning from heterogeneous networks. *Chemical Science*, 11(7):1775–1797, 2020.
- Zhang, Chen, Cheng, Feixiong, Li, Weihua, Liu, Guixia, Lee, Philip W, and Tang, Yun. In silico prediction of drug induced liver toxicity using substructure pattern recognition method. *Molecular informatics*, 35(3-4):136–144, 2016.
- Zhang, Hongyi, Cisse, Moustapha, Dauphin, Yann N, and Lopez-Paz, David. mixup: Beyond empirical risk minimization. *arXiv preprint arXiv:1710.09412*, 2017.
- Zhang, Jingzhao, Menon, Aditya, Veit, Andreas, Bhojanapalli, Srinadh, Kumar, Sanjiv, and Sra, Suvrit. Coping with label shift via distributionally robust optimisation. *arXiv preprint arXiv:2010.12230*, 2020.
- Zhao, Long, Liu, Ting, Peng, Xi, and Metaxas, Dimitris. Maximum-entropy adversarial data augmentation for improved generalization and robustness. In Larochelle, H., Ranzato, M., Hadsell, R., Balcan, M. F., and Lin, H. (eds.), *Advances in Neural Information Processing Systems*, volume 33, pp. 14435–14447. Curran Associates, Inc., 2020.
- Zheng, Shuangjia, Rao, Jiahua, Zhang, Zhongyue, Xu, Jun, and Yang, Yuedong. Predicting retrosynthetic reactions using self-corrected transformer neural networks. *Journal of Chemical Information and Modeling*, 60(1):47–55, 2019.
- Zhou, Chunting, Ma, Xuezhe, Michel, Paul, and Neubig, Graham. Examining and combating spurious features under distribution shift. *arXiv preprint arXiv:2106.07171*, 2021a.
- Zhou, Fan, Jiang, Zhuqing, Shui, Changjian, Wang, Boyu, and Chaib-draa, Brahim. Domain generalization with optimal transport and metric learning. *arXiv preprint arXiv:2007.10573*, 2020a.
- Zhou, Fan, Jiang, Zhuqing, Shui, Changjian, Wang, Boyu, and Chaib-draa, Brahim. Domain generalization via optimal transport with metric similarity learning. *Neurocomputing*, 456(C):469–480, oct 2021b.

Zhou, Kaiyang, Yang, Yongxin, Hospedales, Timothy, and Xiang, Tao. Deep domain-adversarial image generation for domain generalisation. In *Proceedings of the AAAI Conference on Artificial Intelligence*, volume 34, pp. 13025–13032, 2020b.

Zhuang, Fuzhen, Qi, Zhiyuan, Duan, Keyu, Xi, Dongbo, Zhu, Yongchun, Zhu, Hengshu, Xiong, Hui, and He, Qing. A comprehensive survey on transfer learning. *Proceedings of the IEEE*, 109(1):43–76, 2020.

Appendix of DrugOOD

A. Statistics of the Realized Datasets

Table 10: List of 36 lbap datasets in DrugOOD. Pos and Neg denote the numbers of positive and negative data points, respectively. $D^\#$ represents the number of domains, and $C^\#$ represent the number of data points.

Data subset	$Pos^\#$	$Neg^\#$	Train		ID Val		ID Test		OOD Val		OOD Test	
			$D^\#$	$C^\#$	$D^\#$	$C^\#$	$D^\#$	$C^\#$	$D^\#$	$C^\#$	$D^\#$	$C^\#$
DrugOOD-lbap-core-ic50-assay	83802	11434	311	34179	311	11314	311	11683	314	19028	699	19032
DrugOOD-lbap-core-ic50-scaffold	83802	11434	6881	21519	1912	4920	24112	30708	6345	19041	4350	19048
DrugOOD-lbap-core-ic50-size	83802	11434	190	36597	140	12153	229	12411	4	17660	18	16415
DrugOOD-lbap-core-ec50-assay	10199	2462	47	4540	47	1502	47	1557	46	2572	101	2490
DrugOOD-lbap-core-ec50-scaffold	10200	2462	850	2570	224	580	3668	4447	1193	2532	953	2533
DrugOOD-lbap-core-ec50-size	10200	2462	167	4684	103	1513	205	1753	4	2313	17	2399
DrugOOD-lbap-core-ki-assay	22851	488	112	8393	112	2769	112	2900	83	4631	169	4646
DrugOOD-lbap-core-ki-scaffold	22851	488	1820	5323	521	1192	5826	7490	1366	4665	779	4669
DrugOOD-lbap-core-ki-size	22851	488	89	8481	62	2799	118	2941	4	4644	24	4474
DrugOOD-lbap-core-potency-assay	12265	10554	9	8549	9	2848	9	2856	7	4008	65	4558
DrugOOD-lbap-core-potency-scaffold	12032	10787	2003	3361	284	433	8910	9898	2125	4563	1509	4564
DrugOOD-lbap-core-potency-size	11994	10825	48	8629	38	2859	60	2938	3	4182	18	4211
DrugOOD-lbap-refined-ic50-assay	240996	25526	1446	95373	1446	31401	1446	33164	1361	53293	2805	53291
DrugOOD-lbap-refined-ic50-scaffold	240996	25526	19285	60908	5804	14068	66187	84942	15368	53300	9333	53304
DrugOOD-lbap-refined-ic50-size	240996	25526	225	97779	176	32531	264	32847	4	51443	20	51922
DrugOOD-lbap-refined-ec50-assay	32454	5457	141	13600	141	4504	141	4655	186	7586	372	7566
DrugOOD-lbap-refined-ec50-scaffold	32454	5457	2834	7775	745	1647	10945	13324	3082	7587	2187	7578
DrugOOD-lbap-refined-ec50-size	32454	5457	220	13762	140	4524	262	4843	5	8558	17	6224
DrugOOD-lbap-refined-ki-assay	72484	2472	578	26752	578	8765	578	9462	414	14988	905	14989
DrugOOD-lbap-refined-ki-scaffold	72484	2472	5643	17172	1692	3899	18612	23914	4436	15013	2386	14958
DrugOOD-lbap-refined-ki-size	72484	2472	148	28230	102	9366	189	9591	4	13060	23	14709
DrugOOD-lbap-refined-potency-assay	25382	22611	10	17894	10	5962	10	5974	7	8899	105	9264
DrugOOD-lbap-refined-potency-scaffold	25120	22873	4928	8380	850	1145	16819	19270	4344	9598	2927	9600
DrugOOD-lbap-refined-potency-size	25239	22754	51	17951	43	5969	65	6042	4	10731	18	7300
DrugOOD-lbap-general-ic50-assay	476865	91691	6917	201951	6917	65424	6917	73777	6207	113704	16814	113700
DrugOOD-lbap-general-ic50-scaffold	476865	91691	43552	129740	13516	29174	142173	182220	29513	113723	15189	113699
DrugOOD-lbap-general-ic50-size	476865	91691	290	217294	243	72349	311	72742	4	102544	22	103627
DrugOOD-lbap-general-ec50-assay	92445	18000	1079	39333	1079	12849	1079	14086	1137	22095	2883	22082
DrugOOD-lbap-general-ec50-scaffold	92445	18000	8677	23481	2450	4977	30611	37811	7659	22095	4844	22081
DrugOOD-lbap-general-ec50-size	92445	18000	294	42697	238	14151	312	14531	4	19301	20	19765
DrugOOD-lbap-general-ki-assay	146212	6533	2251	54062	2251	17399	2251	20187	1753	30555	4281	30542
DrugOOD-lbap-general-ki-scaffold	146212	6533	12334	34395	3625	7472	39232	49784	8780	30559	4280	30535
DrugOOD-lbap-general-ki-size	146212	6533	190	55386	140	18407	235	18687	5	32508	22	27757
DrugOOD-lbap-general-potency-assay	26784	22389	10	17746	10	5912	10	5926	9	10146	184	9443
DrugOOD-lbap-general-potency-scaffold	25617	23556	5052	8647	887	1196	17122	19660	4565	9834	2674	9836
DrugOOD-lbap-general-potency-size	25674	23499	51	18224	44	6060	66	6138	4	10916	18	7835

Table 11: List of the 60 SBAP datasets in DrugOOD. Pos and Neg denote the numbers of positive and negative data points, respectively. $D^\#$ represents the number of domains and $C^\#$ represent the number of data points.

Data subset	Pos [#]	Neg [#]	Train		ID Val		ID Test		OOD Val		OOD Test	
			D [#]	C [#]								
DrugOOD-sbap-core-ic50-assay	104907	15591	351	43250	351	14327	351	14737	381	24135	723	24049
DrugOOD-sbap-core-ic50-protein	104907	15591	127	43439	127	14449	127	14593	134	24006	416	24011
DrugOOD-sbap-core-ic50-protein-family	104907	15591	1	46890	1	15630	1	15631	2	21112	10	21235
DrugOOD-sbap-core-ic50-scaffold	104907	15591	9911	31201	2560	7149	24334	33948	6151	24138	4322	24062
DrugOOD-sbap-core-ic50-size	104907	15591	192	46390	154	15413	229	15685	4	21422	18	21588
DrugOOD-sbap-core-ec50-assay	12053	3287	55	5541	55	1831	55	1898	53	3023	111	3047
DrugOOD-sbap-core-ec50-protein	12053	3287	29	5524	29	1834	29	1867	28	3109	66	3006
DrugOOD-sbap-core-ec50-protein-family	12053	3287	2	5684	2	1894	2	1897	2	3124	5	2741
DrugOOD-sbap-core-ec50-scaffold	12053	3287	1381	3676	292	761	3680	4768	1154	3068	980	3067
DrugOOD-sbap-core-ec50-size	12053	3287	170	5772	109	1874	205	2130	4	2740	17	2824
DrugOOD-sbap-core-ki-assay	31292	852	164	11540	164	3801	164	3994	116	6427	180	6382
DrugOOD-sbap-core-ki-protein	31292	852	37	11604	37	3858	37	3904	48	6409	125	6369
DrugOOD-sbap-core-ki-protein-family	31292	852	2	16504	2	5501	2	5503			9	4636
DrugOOD-sbap-core-ki-scaffold	31292	852	2712	8640	786	1983	5799	8670	1386	6456	786	6395
DrugOOD-sbap-core-ki-size	31292	852	99	11934	67	3946	118	4094	4	5951	24	6219
DrugOOD-sbap-core-potency-assay	18665	15997	10	12892	10	4295	10	4305	9	6296	63	6874
DrugOOD-sbap-core-potency-protein	19369	15293	9	12699	9	4230	9	4241	7	6568	30	6924
DrugOOD-sbap-core-potency-protein-family	18846	15816	1	15701	1	5233	1	5235	1	4379	6	4114
DrugOOD-sbap-core-potency-scaffold	18665	15997	3460	7891	847	1487	9034	11430	2099	6921	1411	6933
DrugOOD-sbap-core-potency-size	18665	15997	52	13093	46	4352	60	4414	3	6243	18	6560
DrugOOD-sbap-refined-ic50-assay	302752	37178	1760	121655	1760	40060	1760	42245	1712	68003	2937	67967
DrugOOD-sbap-refined-ic50-protein	302752	37178	219	122326	219	40715	219	40992	239	68065	1025	67832
DrugOOD-sbap-refined-ic50-protein-family	302752	37178	1	130685	1	43561	1	43563	2	70150	12	51971
DrugOOD-sbap-refined-ic50-scaffold	302752	37178	28561	89798	7690	20509	65773	93651	14954	67993	8900	67979
DrugOOD-sbap-refined-ic50-size	302752	37178	225	123320	182	41046	264	41357	5	77829	19	56378
DrugOOD-sbap-refined-ec50-assay	35977	6428	177	15205	177	5016	177	5239	212	8484	384	8461
DrugOOD-sbap-refined-ec50-protein	35977	6428	47	15372	47	5112	47	5168	59	8351	195	8402
DrugOOD-sbap-refined-ec50-protein-family	35977	6428	2	18027	2	6008	2	6011	1	4791	8	7568
DrugOOD-sbap-refined-ec50-scaffold	35977	6428	3774	9950	890	2051	10441	13442	2854	8482	1957	8480
DrugOOD-sbap-refined-ec50-size	35977	6428	228	15809	150	5202	262	5527	4	7763	18	8104
DrugOOD-sbap-refined-ki-assay	136133	6050	688	50921	688	16783	688	17628	702	28440	1131	28411
DrugOOD-sbap-refined-ki-protein	136133	6050	125	51209	125	17033	125	17193	121	28364	427	28384
DrugOOD-sbap-refined-ki-protein-family	136133	6050	2	76074	2	25358	2	25359			11	15392
DrugOOD-sbap-refined-ki-scaffold	136133	6050	9870	41972	2878	10685	19006	32687	4194	28531	2009	28308
DrugOOD-sbap-refined-ki-size	136128	6047	164	54637	117	18164	190	18401	4	24120	21	26853
DrugOOD-sbap-refined-potency-assay	39841	32727	13	26983	13	8991	13	9010	7	13315	99	14269
DrugOOD-sbap-refined-potency-protein	39841	32727	12	26411	12	8800	12	8818	7	15531	41	13008
DrugOOD-sbap-refined-potency-protein-family	41827	30741	1	31027	1	10342	1	10344	1	11239	6	9616
DrugOOD-sbap-refined-potency-scaffold	39841	32727	7645	17457	1872	3292	17214	22791	4216	14549	2545	14479
DrugOOD-sbap-refined-potency-size	39840	32726	53	26233	49	8729	65	8810	4	16635	18	12159
DrugOOD-sbap-general-ic50-assay	514296	69105	6171	207522	6171	67554	6171	74982	5678	116671	12019	116672
DrugOOD-sbap-general-ic50-protein	514296	69105	252	209978	252	69923	252	70236	307	116773	2112	116491
DrugOOD-sbap-general-ic50-protein-family	514296	69105	1	224277	1	74759	1	74759	2	122574	12	87032
DrugOOD-sbap-general-ic50-scaffold	514296	69105	50852	156612	14093	35397	109140	158031	24515	116698	12113	116663
DrugOOD-sbap-general-ic50-size	514296	69105	281	226190	233	75318	301	75688	4	102468	22	103737
DrugOOD-sbap-general-ec50-assay	66827	8867	728	26966	728	8805	728	9667	769	15127	1605	15129
DrugOOD-sbap-general-ec50-protein	66827	8867	68	27256	68	9068	68	9158	95	15134	468	15078
DrugOOD-sbap-general-ec50-protein-family	66827	8867	2	31076	2	10358	2	10361	1	12651	10	11248
DrugOOD-sbap-general-ec50-scaffold	66827	8867	6777	18581	1779	3923	17150	22913	4503	15168	2962	15109
DrugOOD-sbap-general-ec50-size	66827	8867	286	27814	228	9195	301	9538	5	16147	20	13000
DrugOOD-sbap-general-ki-assay	264464	14083	3368	98880	3368	32029	3368	36227	2995	55701	5795	55710
DrugOOD-sbap-general-ki-protein	264464	14083	124	100249	124	33386	124	33528	164	55743	948	55641
DrugOOD-sbap-general-ki-protein-family	264464	14083	2	145756	2	48585	2	48588			12	35618
DrugOOD-sbap-general-ki-scaffold	264464	14083	21901	81854	6745	20026	38438	65253	8186	55786	3797	55628
DrugOOD-sbap-general-ki-size	264464	14083	206	104541	159	34782	233	35078	4	48850	22	55296
DrugOOD-sbap-general-potency-assay	40174	33094	13	26972	13	8987	13	9005	8	14494	138	13810
DrugOOD-sbap-general-potency-protein	40174	33094	12	26423	12	8804	12	8820	7	15582	52	13639
DrugOOD-sbap-general-potency-protein-family	42339	30929	1	31218	1	10406	1	10407	1	11240	7	9997
DrugOOD-sbap-general-potency-scaffold	40174	33094	7724	17648	1894	3333	17338	22980	4236	14728	2551	14579
DrugOOD-sbap-general-potency-size	40174	33094	53	26482	49	8813	65	8889	4	16820	18	12264

Table 12: The in-distribution (ID) vs. out of distribution (OOD) of Drug00D lbap datasets trained with empirical risk minimization. The ID test datasets are drawn from the training data with the same distribution, and the OOD test data are distinct from the training data.

Dataset	In-dist	Out-of-Dist	Gap
Drug00D-lbap-core-ic50-assay	89.62 (2.04)	71.98 (0.29)	17.64
Drug00D-lbap-core-ic50-scaffold	87.15 (0.48)	69.54 (0.52)	17.60
Drug00D-lbap-core-ic50-size	92.35 (0.15)	67.48 (0.47)	24.87
Drug00D-lbap-core-ec50-assay	85.23 (0.41)	70.30 (1.45)	14.93
Drug00D-lbap-core-ec50-scaffold	84.86 (0.27)	68.07 (0.68)	16.80
Drug00D-lbap-core-ec50-size	91.47 (0.20)	64.73 (0.55)	26.74
Drug00D-lbap-core-ki-assay	89.10 (3.28)	76.63 (1.64)	12.46
Drug00D-lbap-core-ki-scaffold	83.53 (2.15)	74.11 (2.37)	9.42
Drug00D-lbap-core-ki-size	94.73 (0.74)	71.56 (2.07)	23.17
Drug00D-lbap-core-potency-assay	66.23 (0.50)	53.26 (0.95)	12.97
Drug00D-lbap-core-potency-scaffold	61.83 (0.31)	55.30 (0.72)	6.53
Drug00D-lbap-core-potency-size	67.30 (0.36)	56.84 (1.35)	10.46
Drug00D-lbap-refined-ic50-assay	89.25 (0.64)	72.70 (0.00)	16.55
Drug00D-lbap-refined-ic50-scaffold	86.23 (0.08)	70.45 (0.54)	15.78
Drug00D-lbap-refined-ic50-size	91.31 (0.07)	68.74 (0.37)	22.58
Drug00D-lbap-refined-ec50-assay	76.74 (0.50)	71.05 (1.91)	5.69
Drug00D-lbap-refined-ec50-scaffold	81.10 (0.50)	66.22 (0.34)	14.89
Drug00D-lbap-refined-ec50-size	87.67 (0.29)	62.39 (0.70)	25.28
Drug00D-lbap-refined-ki-assay	90.52 (0.26)	72.48 (1.39)	18.04
Drug00D-lbap-refined-ki-scaffold	82.89 (0.66)	70.11 (2.10)	12.79
Drug00D-lbap-refined-ki-size	89.23 (1.23)	72.44 (0.85)	16.78
Drug00D-lbap-refined-potency-assay	62.99 (0.23)	58.88 (0.51)	4.11
Drug00D-lbap-refined-potency-scaffold	60.54 (0.14)	56.00 (1.29)	4.54
Drug00D-lbap-refined-potency-size	64.94 (0.71)	58.13 (0.49)	6.81
Drug00D-lbap-general-ic50-assay	85.19 (1.15)	69.88 (0.13)	15.32
Drug00D-lbap-general-ic50-scaffold	85.15 (0.24)	67.55 (0.09)	17.60
Drug00D-lbap-general-ic50-size	89.77 (0.08)	66.05 (0.32)	23.72
Drug00D-lbap-general-ec50-assay	83.32 (0.60)	69.55 (0.44)	13.77
Drug00D-lbap-general-ec50-scaffold	80.12 (0.44)	63.66 (0.37)	16.46
Drug00D-lbap-general-ec50-size	86.22 (0.23)	62.67 (0.47)	23.55
Drug00D-lbap-general-ki-assay	87.98 (1.34)	74.54 (0.46)	13.44
Drug00D-lbap-general-ki-scaffold	81.05 (3.11)	70.35 (0.83)	10.69
Drug00D-lbap-general-ki-size	89.51 (0.88)	71.29 (0.94)	18.22
Drug00D-lbap-general-potency-assay	63.40 (0.39)	56.38 (0.72)	7.03
Drug00D-lbap-general-potency-scaffold	61.56 (0.29)	56.57 (0.42)	4.99
Drug00D-lbap-general-potency-size	65.15 (0.30)	57.32 (0.54)	7.83

Table 13: The in-distribution (ID) vs. out of distribution (OOD) of Drug00D sbap datasets trained with empirical risk minimization. The ID test dataset are drawn from the training data with the same distribution, and the OOD test data are distinct from the training data.

Dataset	In-dist	Out-of-Dist	Gap
Drug00D-sbap-core-ic50-assay	91.32 (0.40)	71.04 (0.51)	20.28
Drug00D-sbap-core-ic50-protein	90.71 (0.29)	68.87 (0.53)	21.84
Drug00D-sbap-core-ic50-protein-family	89.88 (1.44)	72.20 (0.14)	17.68
Drug00D-sbap-core-ic50-scaffold	88.97 (0.13)	70.73 (0.34)	18.24
Drug00D-sbap-core-ic50-size	92.83 (0.07)	67.17 (0.16)	25.66
Drug00D-sbap-core-ec50-assay	87.57 (0.80)	75.67 (1.34)	11.89
Drug00D-sbap-core-ec50-protein	87.21 (0.78)	69.62 (4.45)	17.59
Drug00D-sbap-core-ec50-protein-family	92.67 (0.94)	56.01 (3.03)	36.66
Drug00D-sbap-core-ec50-scaffold	87.60 (0.32)	69.26 (1.20)	18.34
Drug00D-sbap-core-ec50-size	92.98 (0.30)	63.99 (1.36)	28.98
Drug00D-sbap-core-ki-assay	88.34 (4.18)	63.17 (2.46)	25.16
Drug00D-sbap-core-ki-protein	85.05 (4.48)	64.89 (1.95)	20.16
Drug00D-sbap-core-ki-scaffold	85.96 (1.10)	70.03 (2.90)	15.93
Drug00D-sbap-core-ki-size	92.76 (0.18)	69.68 (1.13)	23.09
Drug00D-sbap-core-potency-assay	70.22 (0.24)	51.39 (0.45)	18.83
Drug00D-sbap-core-potency-protein	70.72 (0.48)	54.62 (0.57)	16.10
Drug00D-sbap-core-potency-protein-family	62.60 (3.47)	49.83 (1.99)	12.77
Drug00D-sbap-core-potency-scaffold	63.36 (0.55)	56.87 (0.53)	6.49
Drug00D-sbap-core-potency-size	66.94 (0.37)	58.36 (0.23)	8.59
Drug00D-sbap-refined-ic50-assay	88.07 (1.48)	69.21 (0.29)	18.86
Drug00D-sbap-refined-ic50-protein	86.87 (1.41)	69.51 (0.30)	17.36
Drug00D-sbap-refined-ic50-protein-family	86.44 (3.07)	70.61 (0.42)	15.82
Drug00D-sbap-refined-ic50-scaffold	87.16 (0.08)	70.10 (0.52)	17.06
Drug00D-sbap-refined-ic50-size	90.22 (0.11)	65.23 (0.26)	24.99
Drug00D-sbap-refined-ec50-assay	80.60 (1.69)	70.38 (1.38)	10.22
Drug00D-sbap-refined-ec50-protein	81.62 (1.16)	73.45 (1.67)	8.17
Drug00D-sbap-refined-ec50-protein-family	83.09 (0.73)	68.81 (1.62)	14.27
Drug00D-sbap-refined-ec50-scaffold	82.44 (0.19)	68.45 (0.28)	13.99
Drug00D-sbap-refined-ec50-size	87.20 (0.04)	64.56 (0.51)	22.64
Drug00D-sbap-refined-ki-assay	96.35 (0.56)	68.00 (1.73)	28.35
Drug00D-sbap-refined-ki-protein	94.22 (0.48)	77.77 (0.60)	16.46
Drug00D-sbap-refined-ki-scaffold	88.27 (0.88)	59.81 (1.04)	28.46
Drug00D-sbap-refined-ki-size	91.56 (0.41)	61.64 (2.41)	29.92
Drug00D-sbap-refined-potency-assay	64.65 (0.11)	54.66 (0.79)	9.99
Drug00D-sbap-refined-potency-protein	65.46 (0.42)	53.14 (0.35)	12.32
Drug00D-sbap-refined-potency-protein-family	64.76 (0.88)	53.75 (0.82)	11.01
Drug00D-sbap-refined-potency-scaffold	61.90 (0.28)	55.05 (0.40)	6.85
Drug00D-sbap-refined-potency-size	64.64 (0.65)	55.79 (0.26)	8.85
Drug00D-sbap-general-ic50-assay	87.85 (1.47)	68.61 (0.54)	19.24
Drug00D-sbap-general-ic50-protein	85.34 (1.67)	68.48 (0.27)	16.86
Drug00D-sbap-general-ic50-protein-family	79.18 (2.69)	68.60 (0.68)	10.58
Drug00D-sbap-general-ic50-scaffold	84.33 (0.67)	67.49 (0.33)	16.84
Drug00D-sbap-general-ic50-size	87.81 (0.23)	65.34 (0.38)	22.47
Drug00D-sbap-general-ec50-assay	84.66 (1.32)	69.83 (0.54)	14.82
Drug00D-sbap-general-ec50-protein	82.10 (0.51)	70.16 (0.29)	11.94
Drug00D-sbap-general-ec50-protein-family	83.69 (1.74)	63.76 (1.05)	19.93
Drug00D-sbap-general-ec50-scaffold	82.97 (0.51)	67.95 (0.27)	15.01
Drug00D-sbap-general-ec50-size	87.98 (0.42)	65.64 (0.35)	22.33
Drug00D-sbap-general-ki-assay	94.15 (0.31)	72.05 (0.49)	22.10
Drug00D-sbap-general-ki-protein	90.72 (0.14)	74.41 (0.25)	16.31
Drug00D-sbap-general-ki-scaffold	87.09 (0.34)	67.36 (1.52)	19.73
Drug00D-sbap-general-ki-size	91.10 (0.26)	65.93 (1.13)	25.17
Drug00D-sbap-general-potency-assay	65.68 (0.17)	53.31 (0.32)	12.36
Drug00D-sbap-general-potency-protein	64.83 (0.77)	53.35 (0.33)	11.48
Drug00D-sbap-general-potency-protein-family	61.28 (0.87)	55.46 (1.24)	5.82
Drug00D-sbap-general-potency-scaffold	61.91 (0.84)	56.02 (0.27)	5.89
Drug00D-sbap-general-potency-size	65.80 (0.13)	55.33 (0.38)	10.47